Managing the Interdisciplinary Requirements of 3D Geological Models
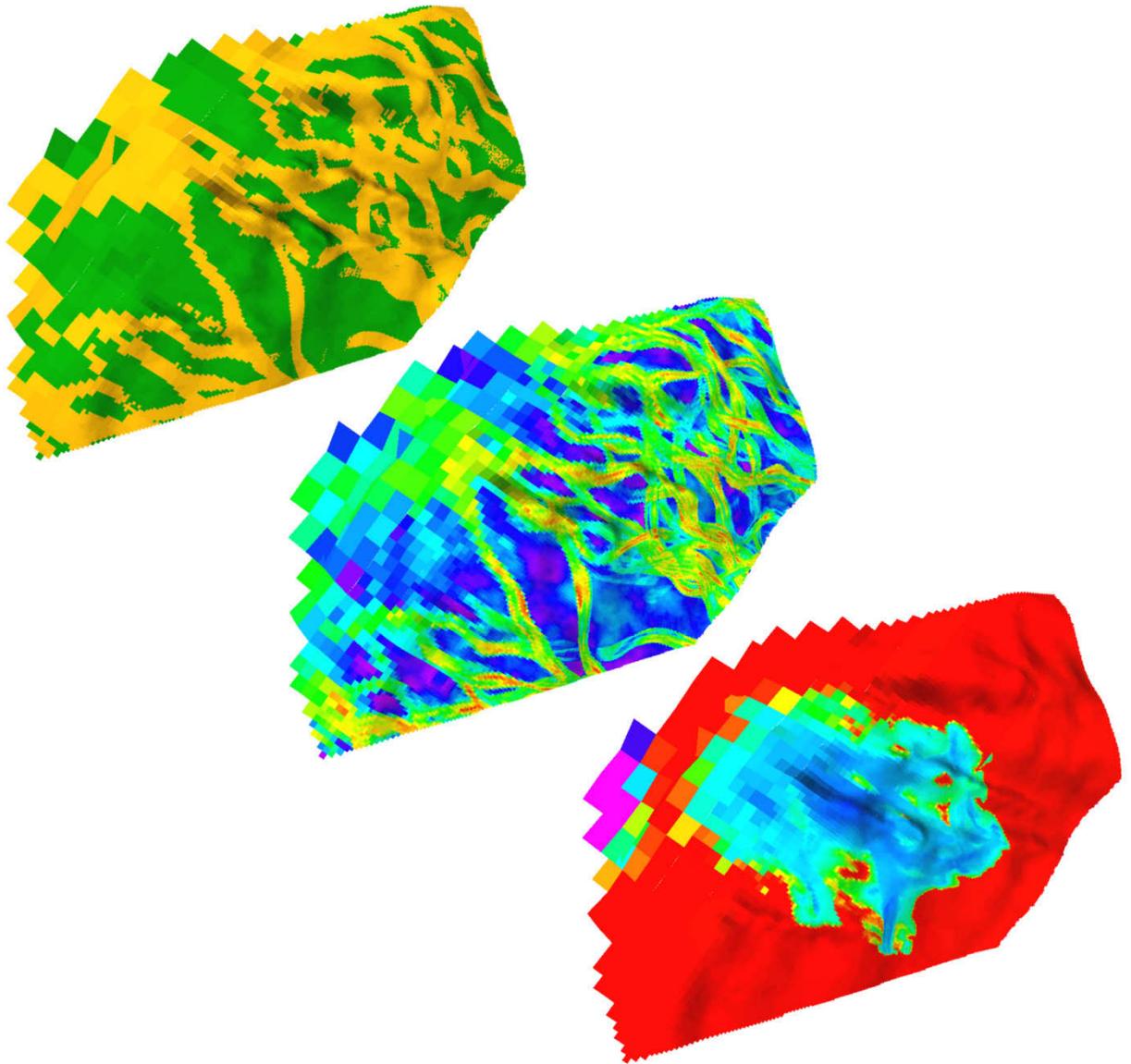
Sarah Jane Riordan
Australian School of Petroleum
University of Adelaide
March 2009

THE UNIVERSITY OF ADELAIDE AUSTRALIA

SUB CRUCE LUMEN

ASP
Australian School of Petroleum

Thesis submitted in accordance with the requirements of the University of Adelaide

for the degree of Doctor in Philosophy
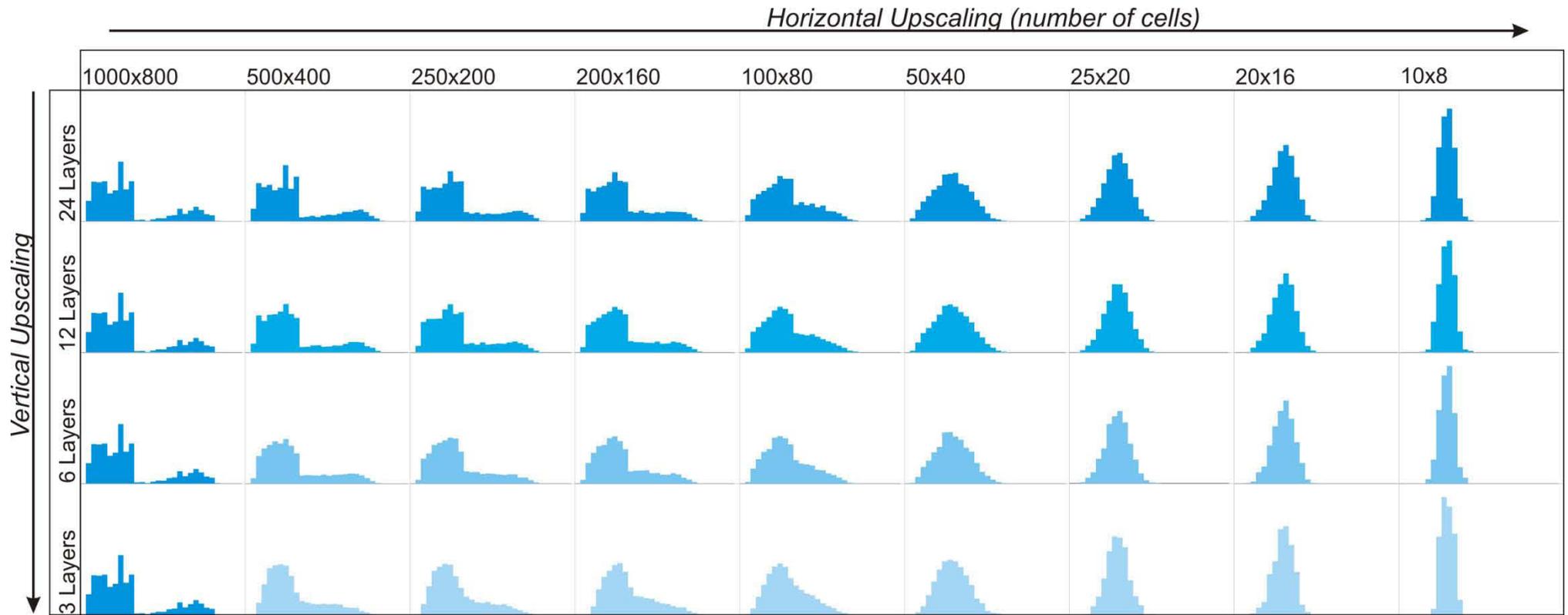
Figure 5.18. Silhouettes of the porosity distributions for all grids. SQ100-25 scenario. The influence of horizontal upscaling is clearly seen by following the changes in silhouette from left to right in any of the levels. The impact of vertical averaging can be seen by following the changes from top to bottom, especially in the more detailed grids on the left side of the diagram. The impact of vertical averaging is not as profound as that of the horizontal upscaling as the channel thickness is not fully exceeded, even by the 3-layer model. It is anticipated that if it were, the bimodal nature of the fine (x & y) models would tend towards a normal distribution.
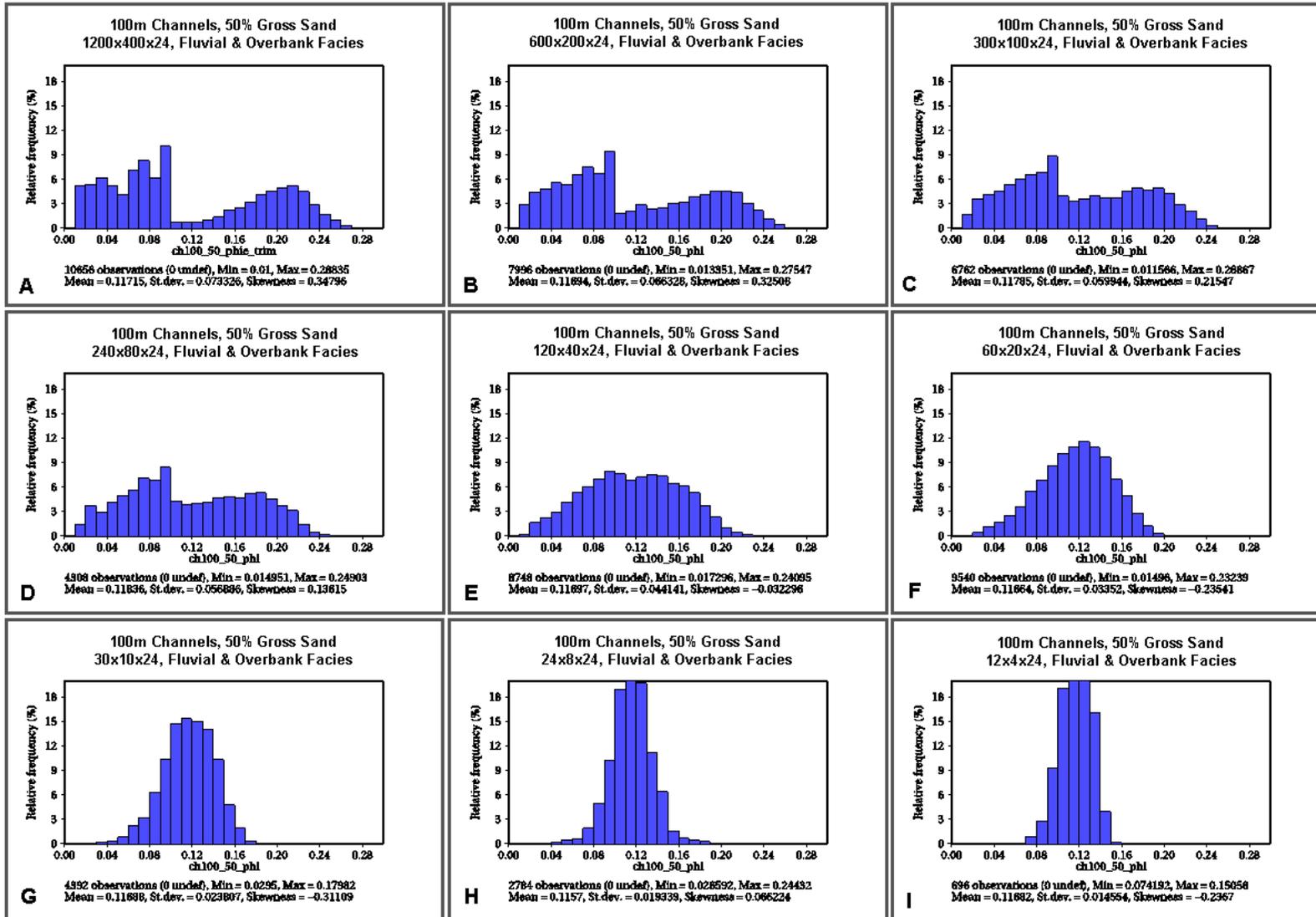
Figure 5.19. Histogram of porosity values for the 24 layer SDA100-50 scenario. Cell width exceeds channel width between diagrams D and E. As with the channel scenarios with 25% gross sand, the distribution starts to tend towards a normal distribution once the cell width exceeds the channel width.
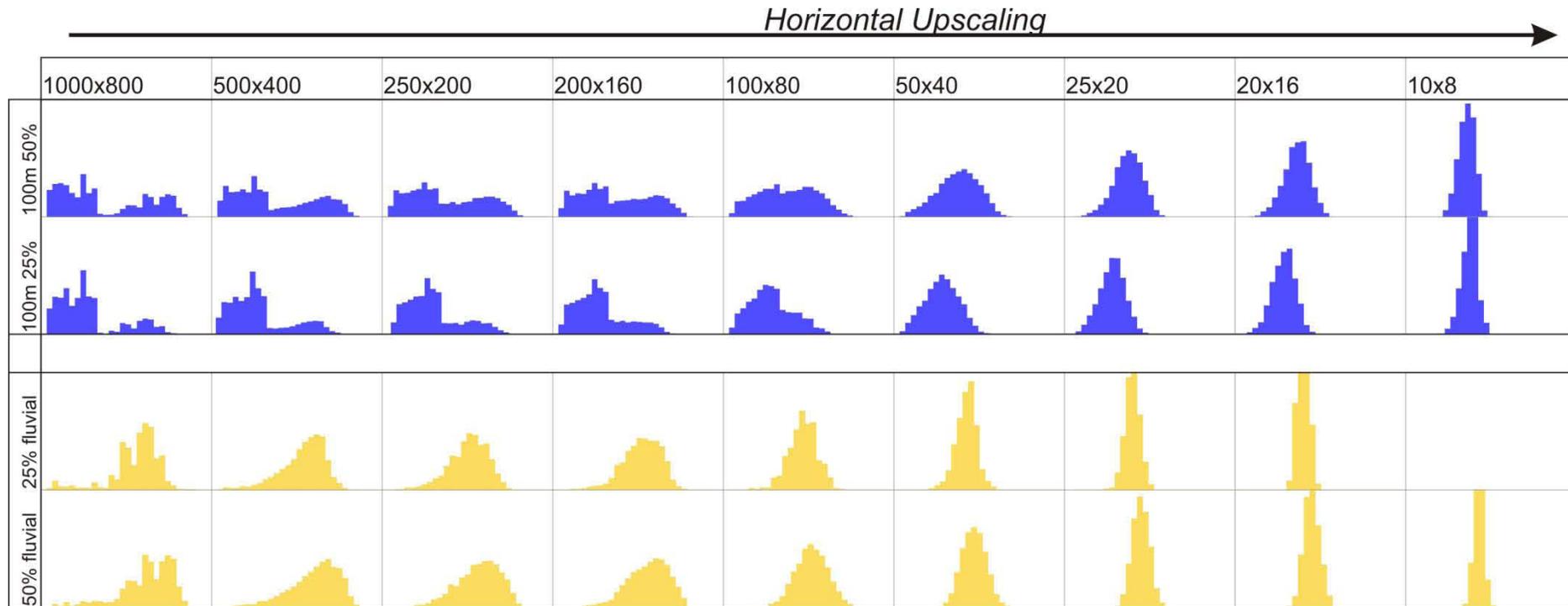
Figure 5.20. A comparison of the porosity distribution of the 25% and 50% gross sand, 100 m channel scenarios (square grid). The blue histograms contain data for both the fluvial and overbank facies. The yellow histograms contain only data for the fluvial facies. Although the histograms for the whole grid (blue) look different between the two scenarios, the distribution of the fluvial facies is similar. Both scenarios show a change form a lognormal distribution to a normal distribution of the fluvial facies between the 200 x 160 and the 100 x 80 grids. These two grids represent the point at which the cell width becomes larger than the channel width.
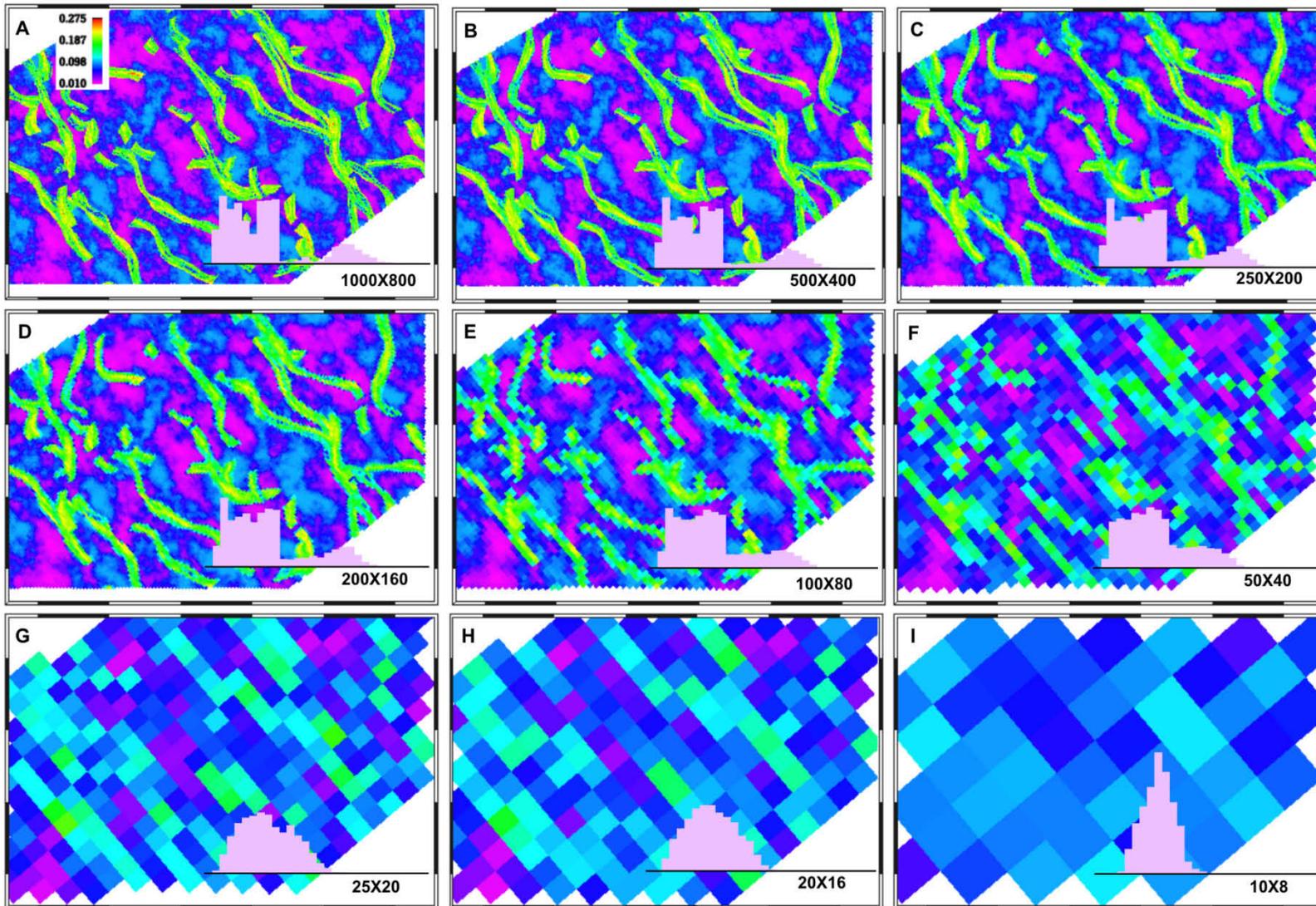
Figure 5.21. Porosity model and histogram of SQ280-25 scenario, 24 layers. As the porosity grids are upscaled the edges of channels become blurred, and once the channel width is smaller than the cell size (G) the channels are no longer visible. This visual change is reflected in the porosity distribution histograms (purple) for each model.
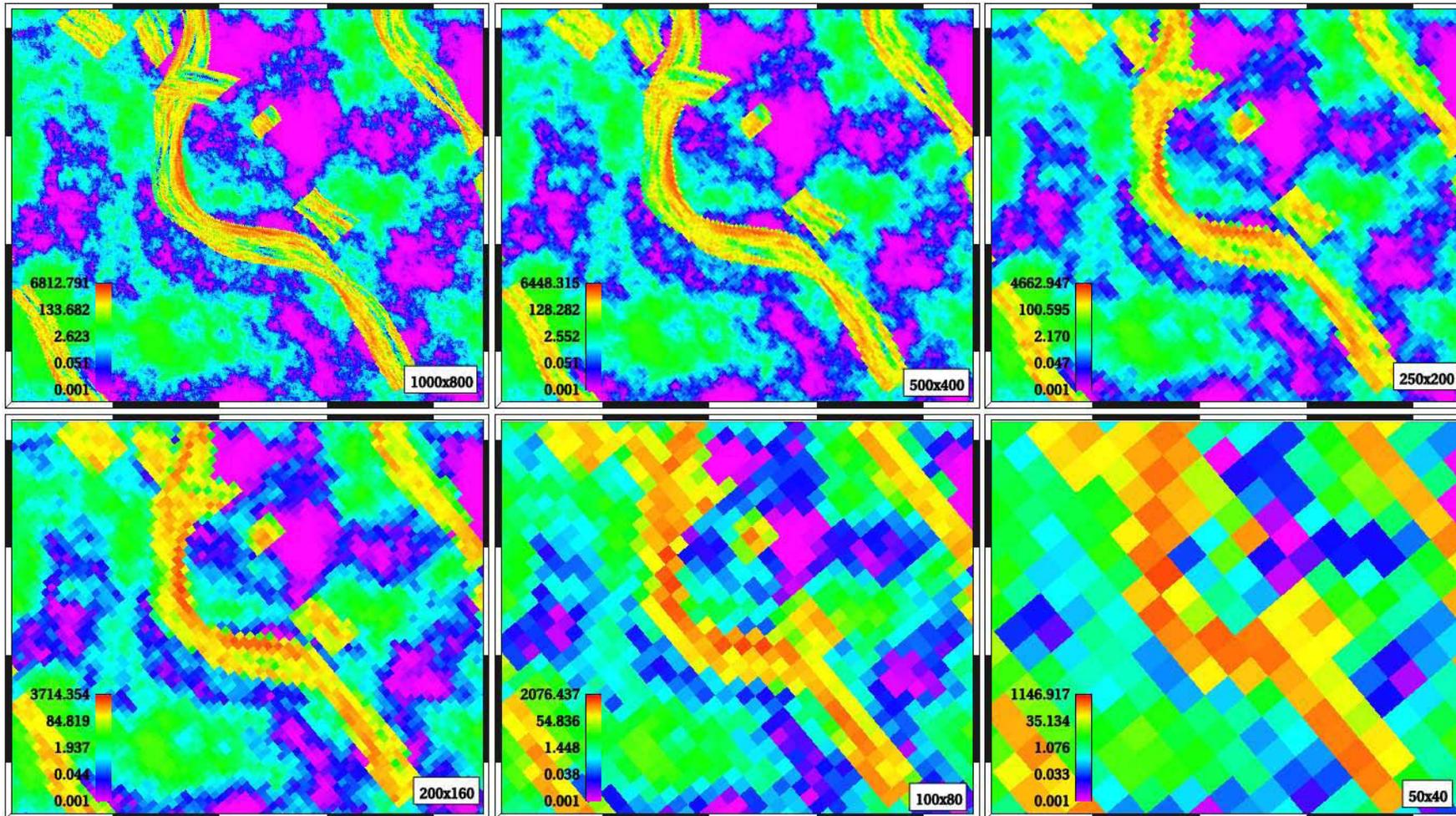
Figure 5.22. Upscaling high permeability streaks in 280 m wide channels—square grid design. The thin permeability streaks (red) in the channel were built using a variogram with a width of 100 m, thus the majority of permeability streaks are less than or equal to 100 m wide. The width of the permeability streak is exceeded in the 100 x 80 m grid, whilst the channel width is not equaled until the 50 x 40 grid. It can be seen that the permeability streak looses definition before the channel thickness is reached. If maintaining the detail of thin features such as permeability streaks or baffles is critical, then the dimensions of the variograms used to construct the petrophysical models need to be considered when deciding on cell dimensions.
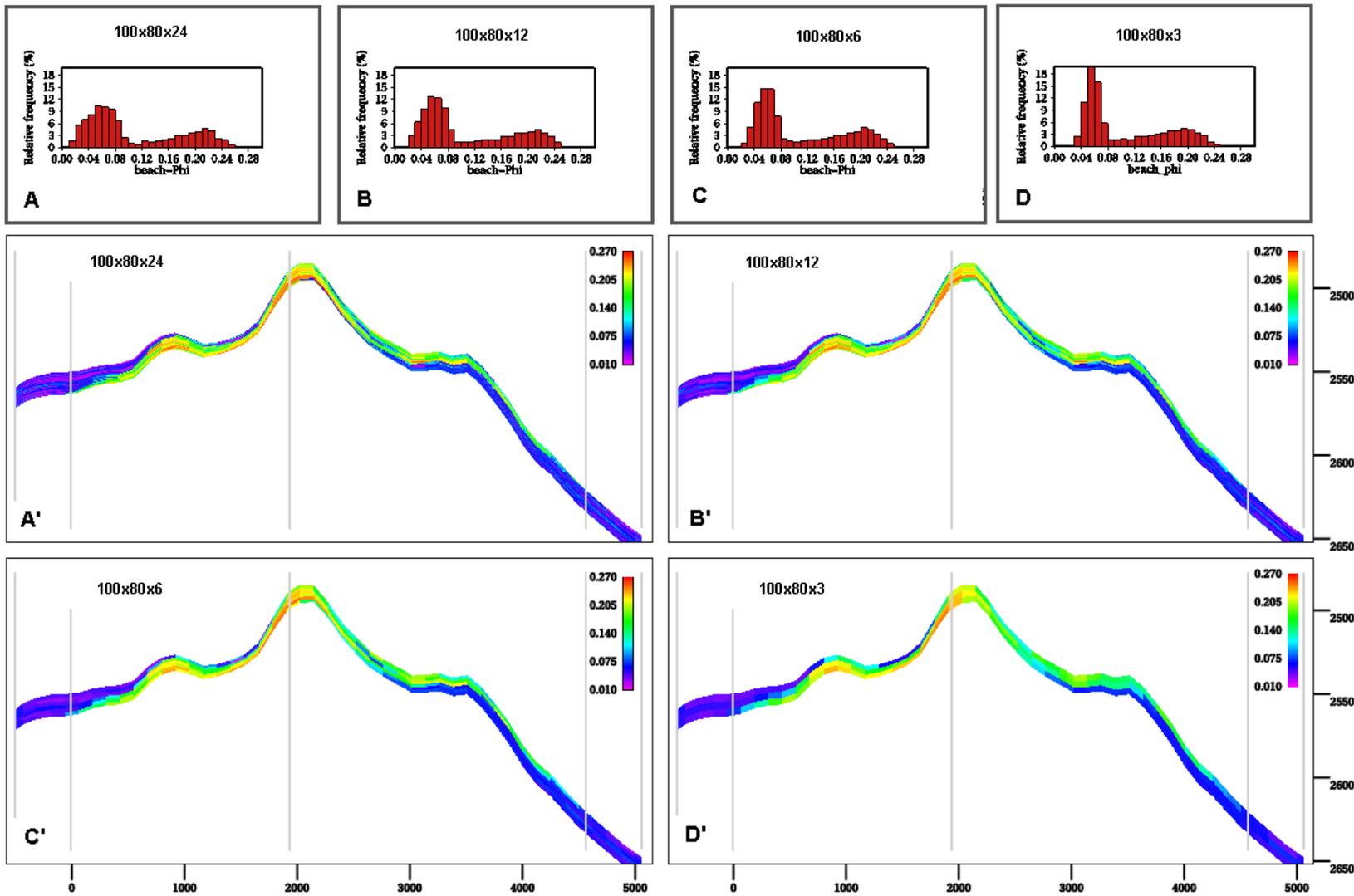
Figure 5.23. Vertical upscaling of porosity in the beach scenario. 100 x 180 cells. The vertical upscaling from 24 to 3 layers does not significantly affect the interface between the low porosity offshore and coastal plain facies (purple) and the high porosity shoreface (red to green). The histograms indicate that within each facies the porosity distribution is narrowing with upscaling.
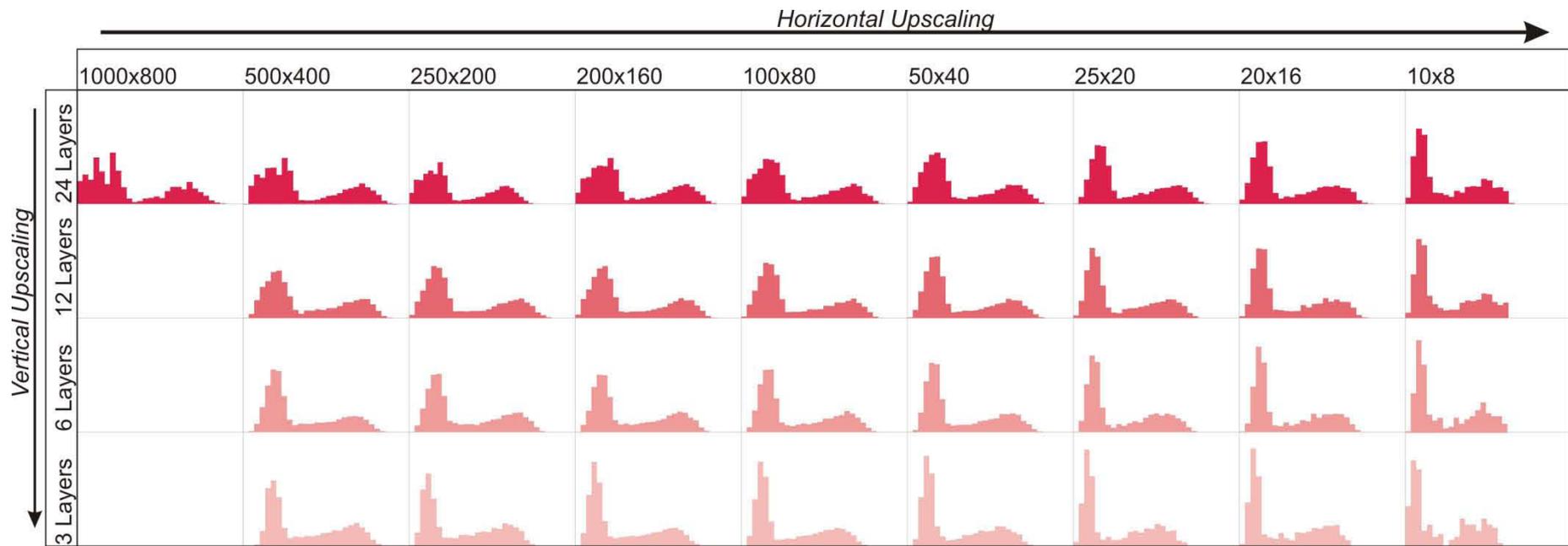
Figure 5.24. Porosity distribution for the SQ beach scenario, all layers. This scenario consists of offshore, shoreface and coastal plain facies only. This highlights the porosity distribution as a result of both vertical and horizontal upscaling. Unlike the channel models, the bimodal nature of the distribution does not change, indicating that there is no significant blending of facies and their associated porosity distributions as a result of the upscaling process. Changes to curves are the result of averaging affects within the facies datasets.
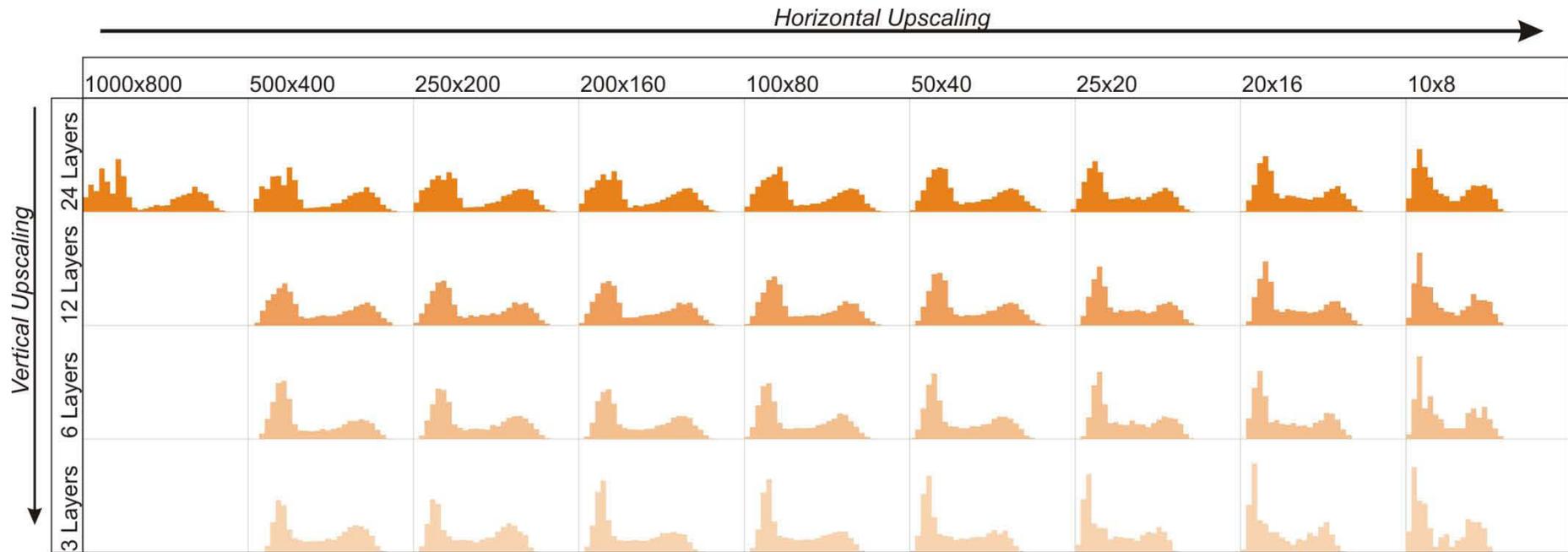
Figure 5.25. Histograms of porosity distribution in the SQ coast scenario. All models retain the original bimodal distribution. As shown in Figure 5.28 the influence of the fluvial facies increases once the width of the cells exceeds the width of the channels (25 x 20 grids).
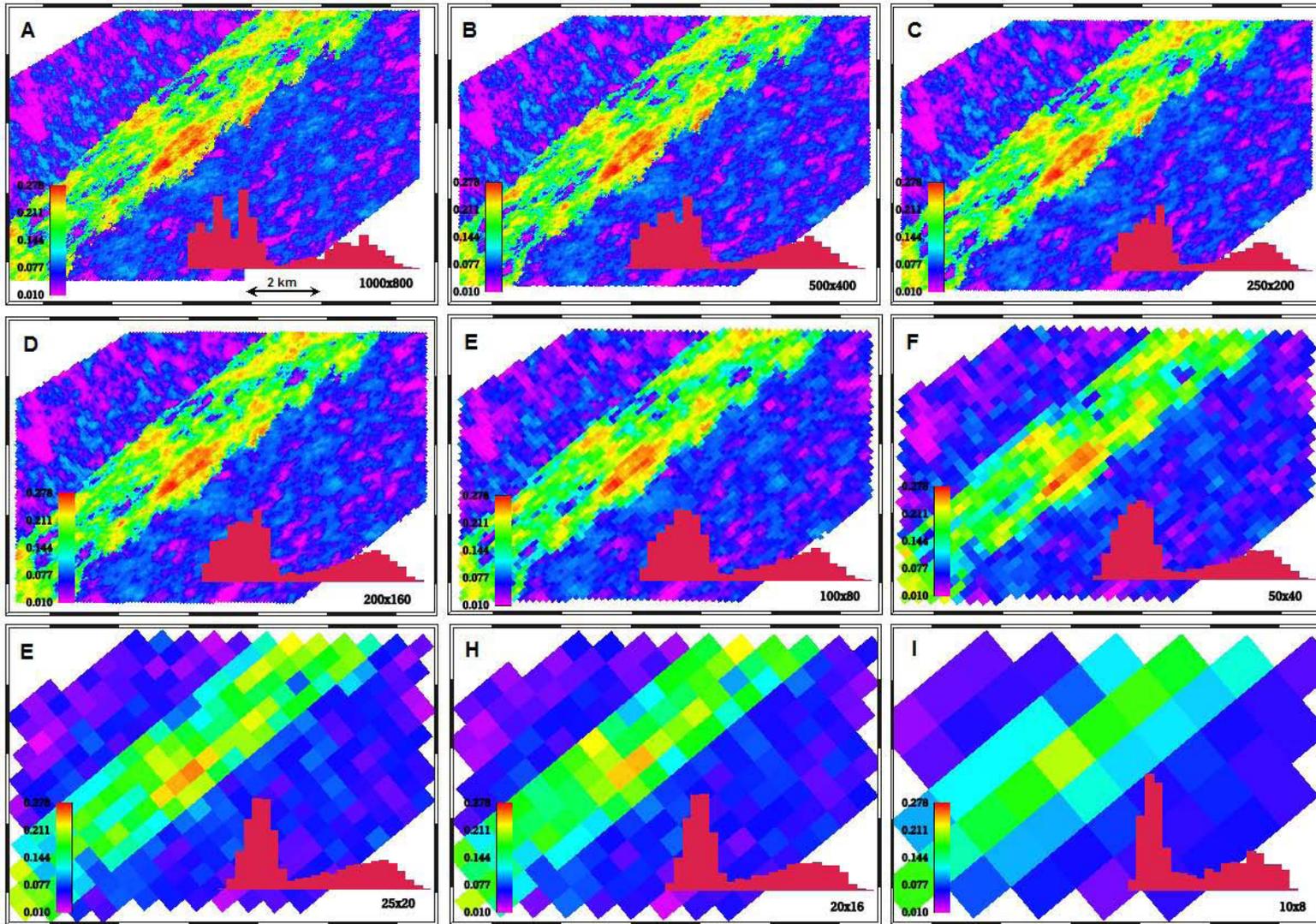
Figure 5.26. Porosity model—SQ beach scenario. 24 layers. The porosity distribution for this scenario is bimodal. All the high porosity values are in the shoreface facies, while the majority of the low porosity values are in the offshore and coastal plain facies. These diagrams highlight the need to consider the porosity distributions during upscaling as well as the facies boundaries. The outline of the shoreface is preserved in all models except the 10 x 8 grid (I). However, resolution of the porosity sweet spots (red) is lost when the grid is 25 x 20 cell (E). At this point the width of sweet spots is matched or exceeded.
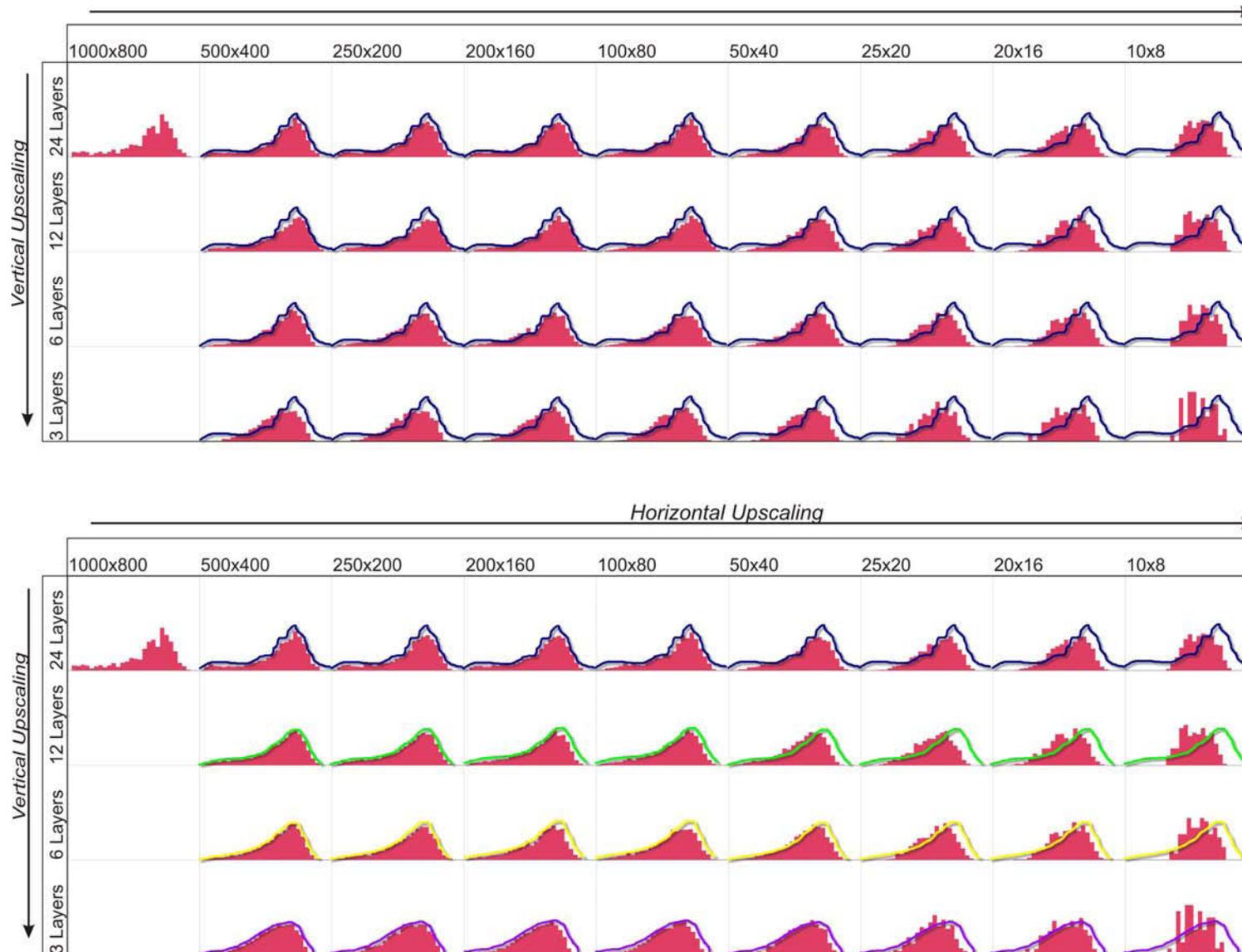
Figure 5.27. Porosity distribution of the shoreface component of the beach scenario (square grid). The top array shows the change in porosity distribution relative to the 500 x 400 x 24 grid (blue outlines). This highlights the influence of vertical upscaling on the porosity distribution. The bottom array shows the changes in porosity distribution relative to the 500 x 400 grid for each vertical upscale step (12 layers etc). This highlights that relative to that grid there is not much change between upscaled grid until the 50 x 40 grid for all layer designs.
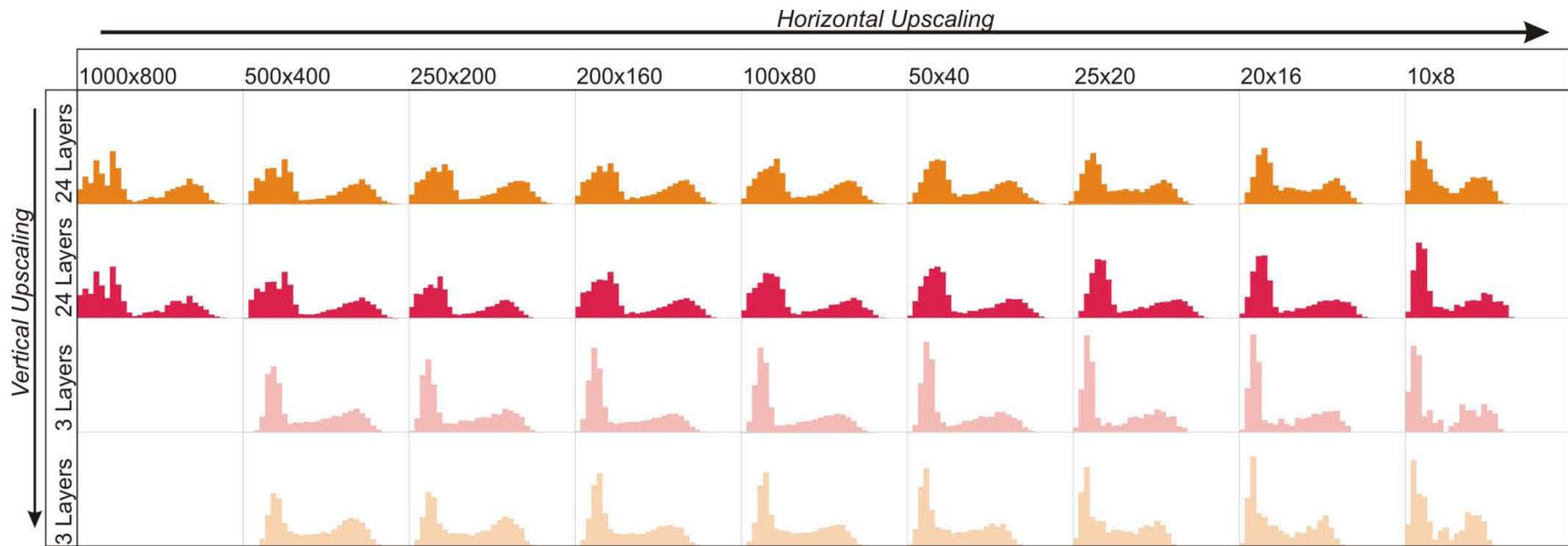
Figure 5.28. A comparison of the 'beach' and 'coast' porosity distributions—square grid. The 'beach' models (red/pink) show relatively little change in distribution pattern with horizontal upscaling until the final model (10 x 8) is reached. There are differences between the 24-layer and -layer models that persist through all the 3-layer models, indicating that any upscaling to this level will change the distribution from the original 1000 x 800 x 24 model. The 'coast model (orange) shows a subtle change in the porosity distribution in the 25 x 20 models to a trimodal distribution. The centre portion of the histogram flattens and shows the beginnings of a new bump. The fluvial channels are 280 m wide—the same width as the cells in the 50 x 40 model. Thus, as was seen in the 280 m channel scenarios, upscaling the grid beyond the width of thee channel facies has an impact of the porosity distribution of the model. These changes in distribution in the grids with fewer than 50 x 40 cells is more pronounced in the 3-layer model.
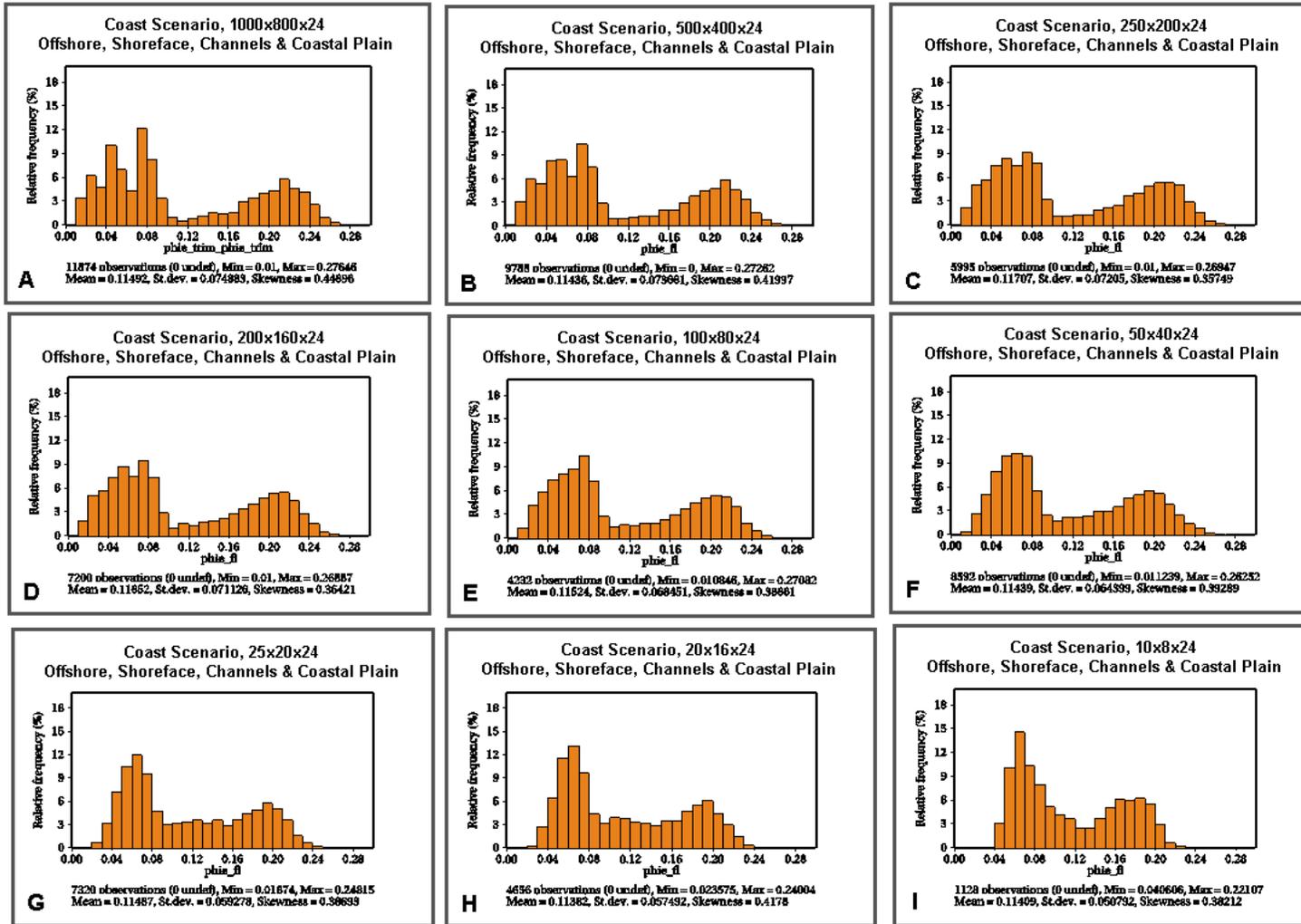
Figure 5.29. Porosity distribution—SQ coast' scenario, 24 layers. The distributions are similar to the base grid (A) until the 25 x 20 grid (G). At this point the cell width exceeds that channel width and the distribution of the porosity in the channel facies begin. This is reflected in the appearance of the beginning of a third hump in the middle of the histogram (around 0.12). The majority of change occurs in the sub 10% potion, which mainly represents the offshore and coastal plain facies. Figure 5.31 shows the shoreface facies porosity—which highlights the stability of the shoreface porosity distribution up to the 50 x 40 grid. See following figures for porosity distribution by facies.
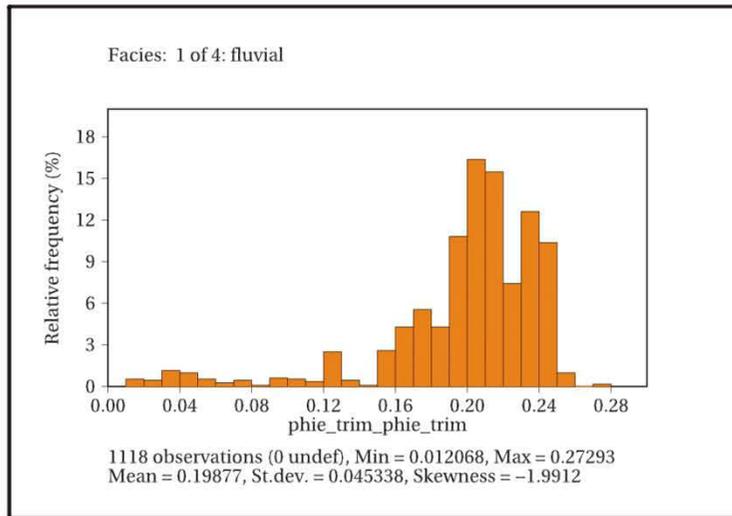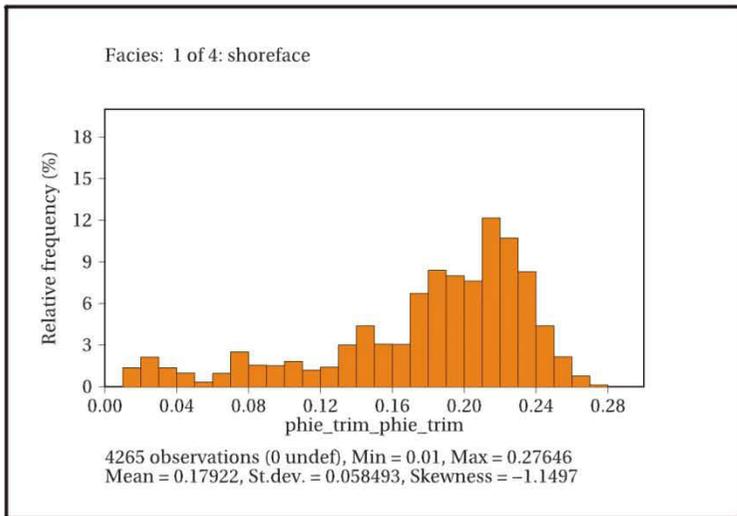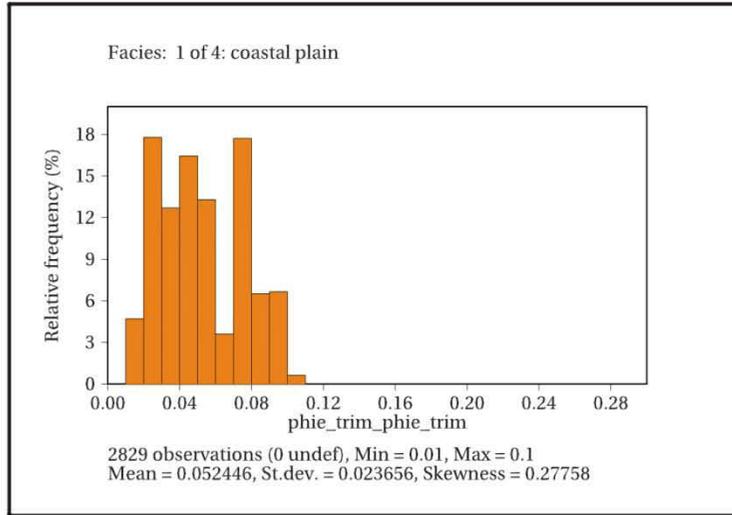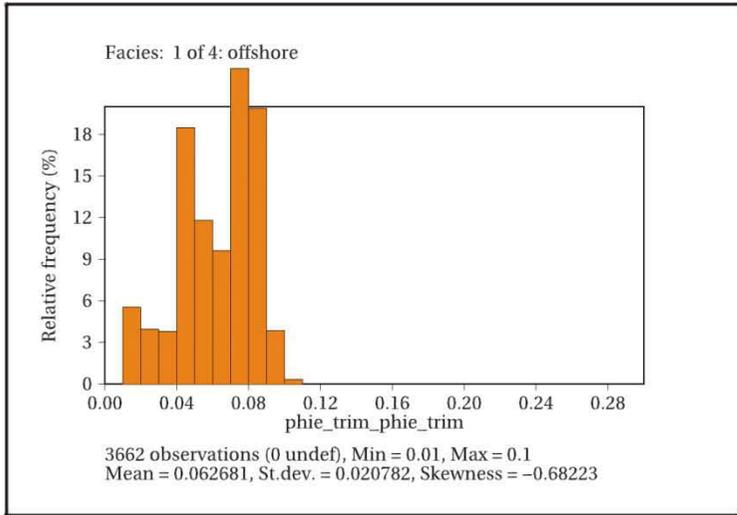
Figure 5.30. Breakdown of porosity distribution for SQ coast' scenario by facies. 1000 x 800 x 24 model. Although the range of porosity values in the shoreface and channel facies is very similar, their distribution is not. The fluvial facies is dominated by porosity values between 16% and 25%, whilst the shoreface facies has a significant amount of values less than 16%.
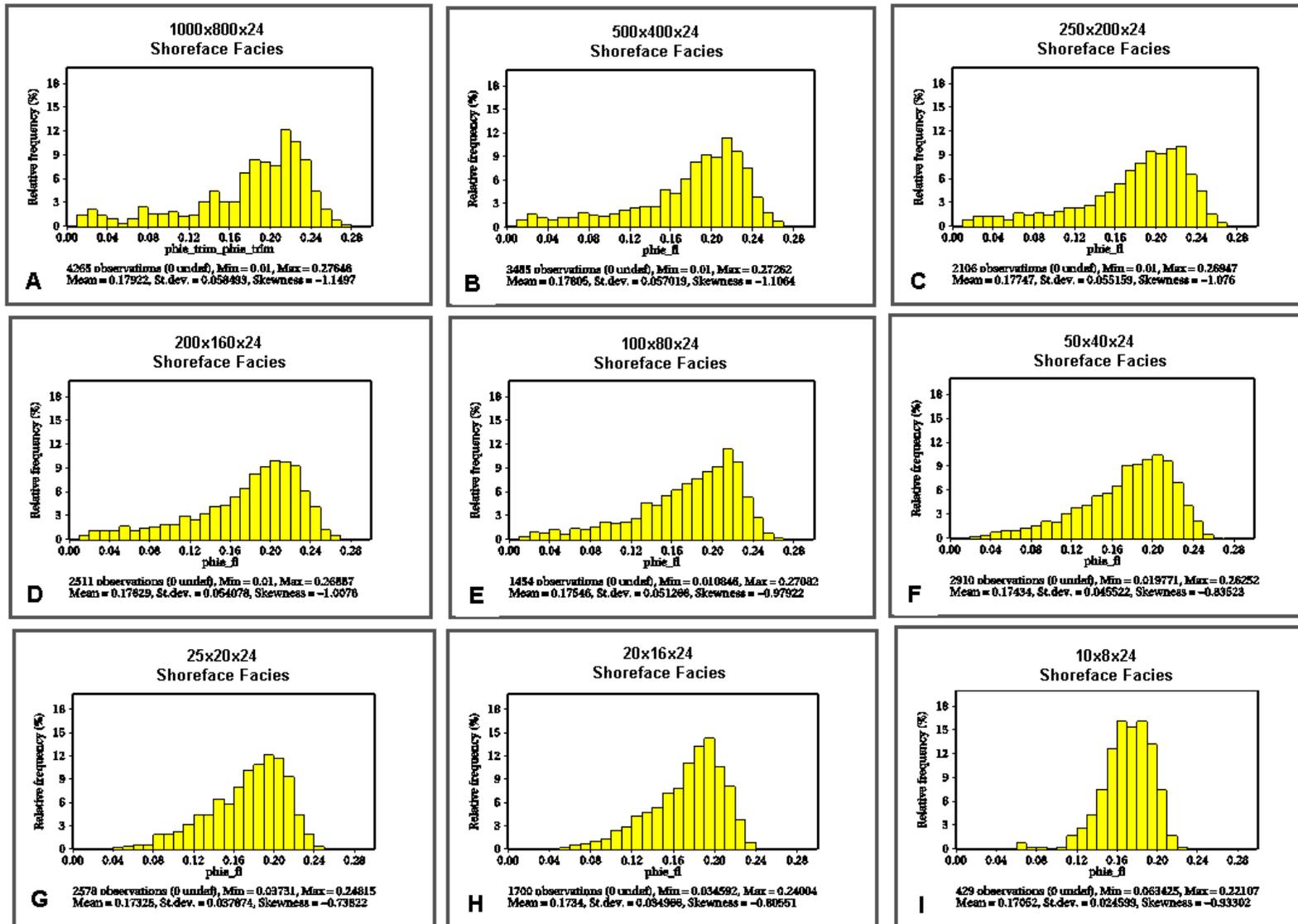
Figure 5.31. SQ coast scenario - Shoreface facies porosity distribution. The distribution of porosity values in the shoreface facies remains lognormal for all upscaled grids except the last (I).
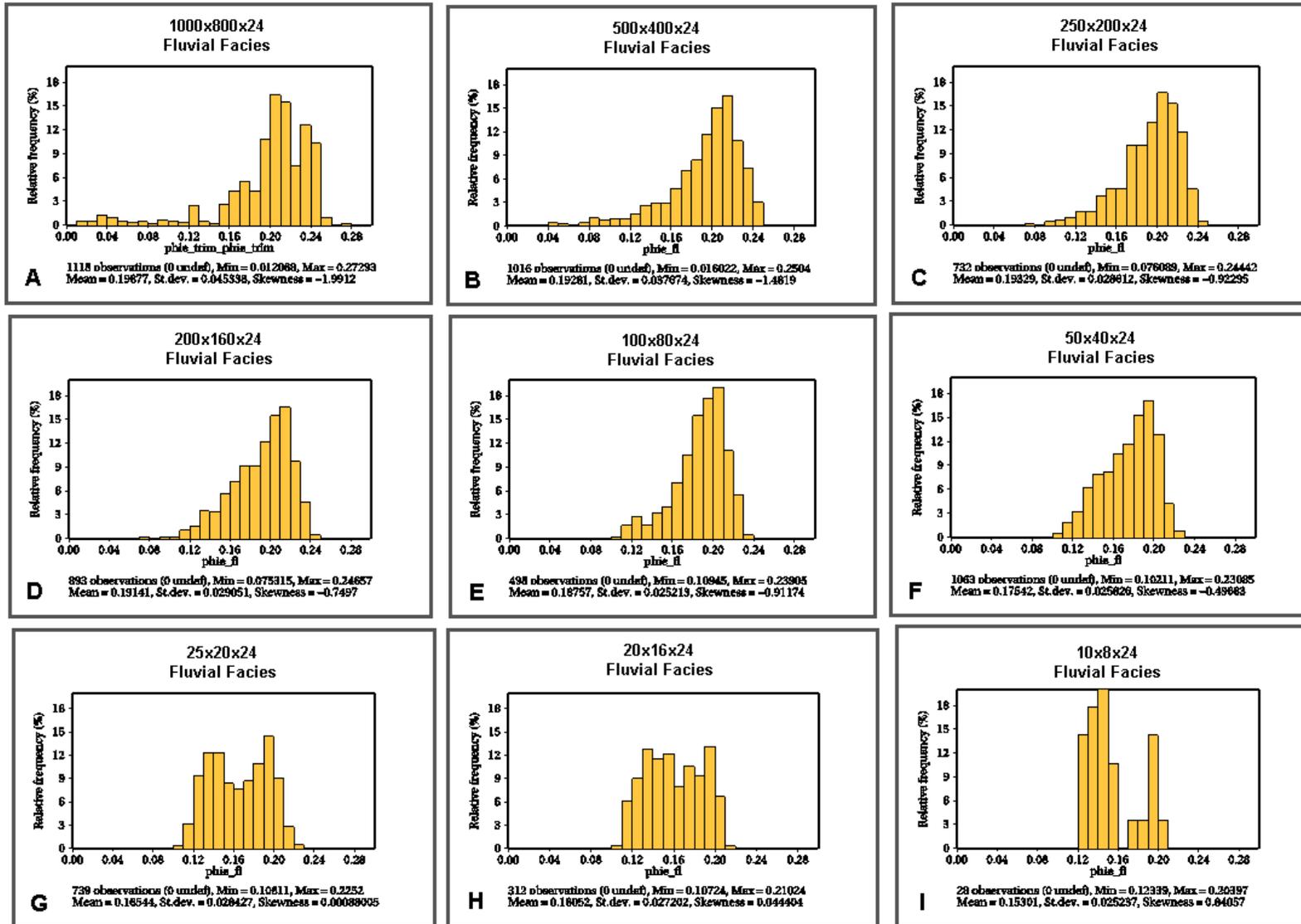
Figure 5.32. Porosity distribution in the fluvial facies in the SQ coast scenario. The channel width of 280 m is the same as the cell width in the 50 x 40 grid. Once the model has been upscaled beyond this grid size, the porosity distribution changes significantly.
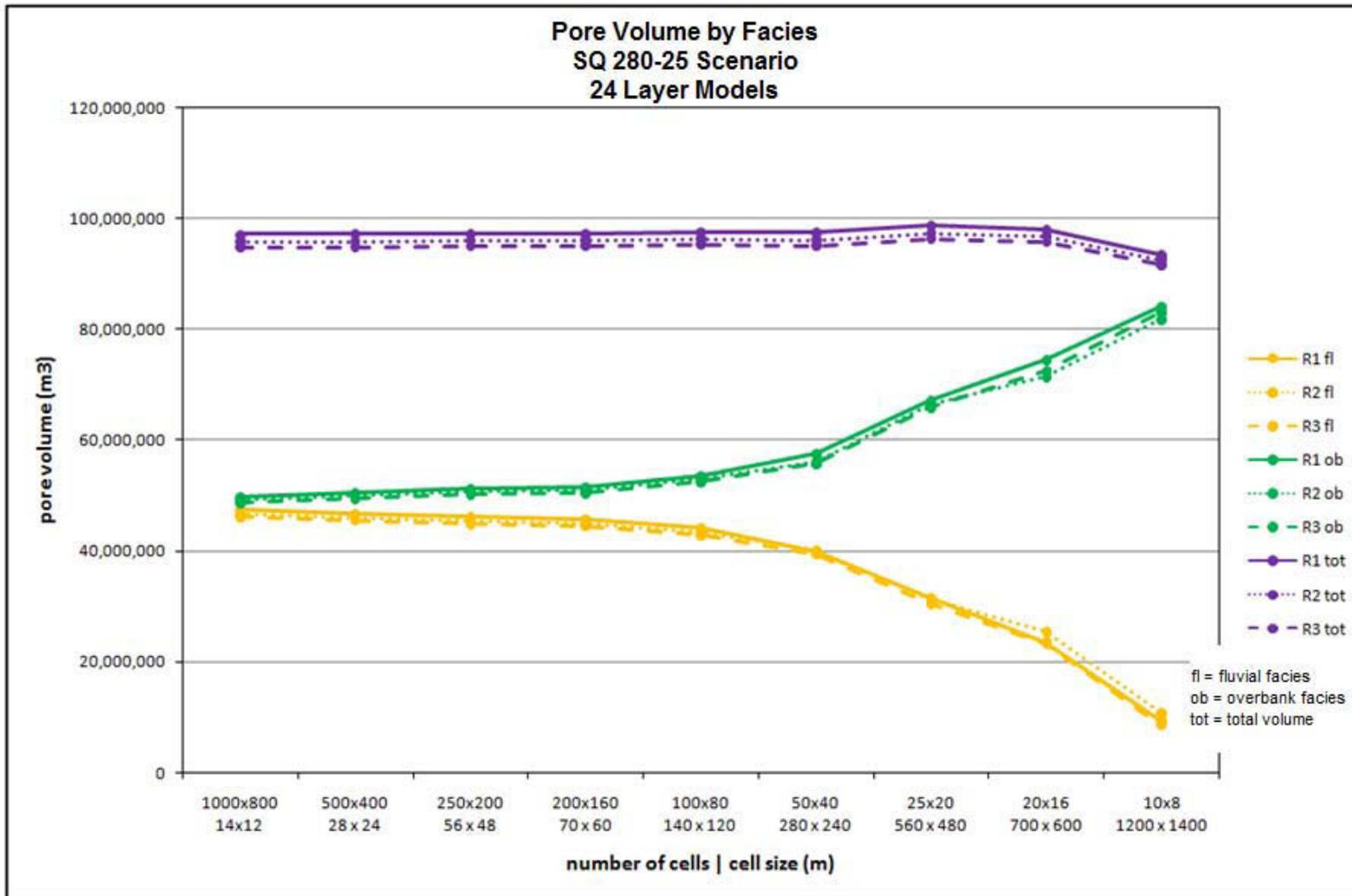
Figure 5.33. Pore volume by facies (fl: fluvial, ob: overbank, tot: total pore volume). 24 layers, SQ 280-25 scenario. Three realizations have very similar pore volumes associated with each facies for every grid design.
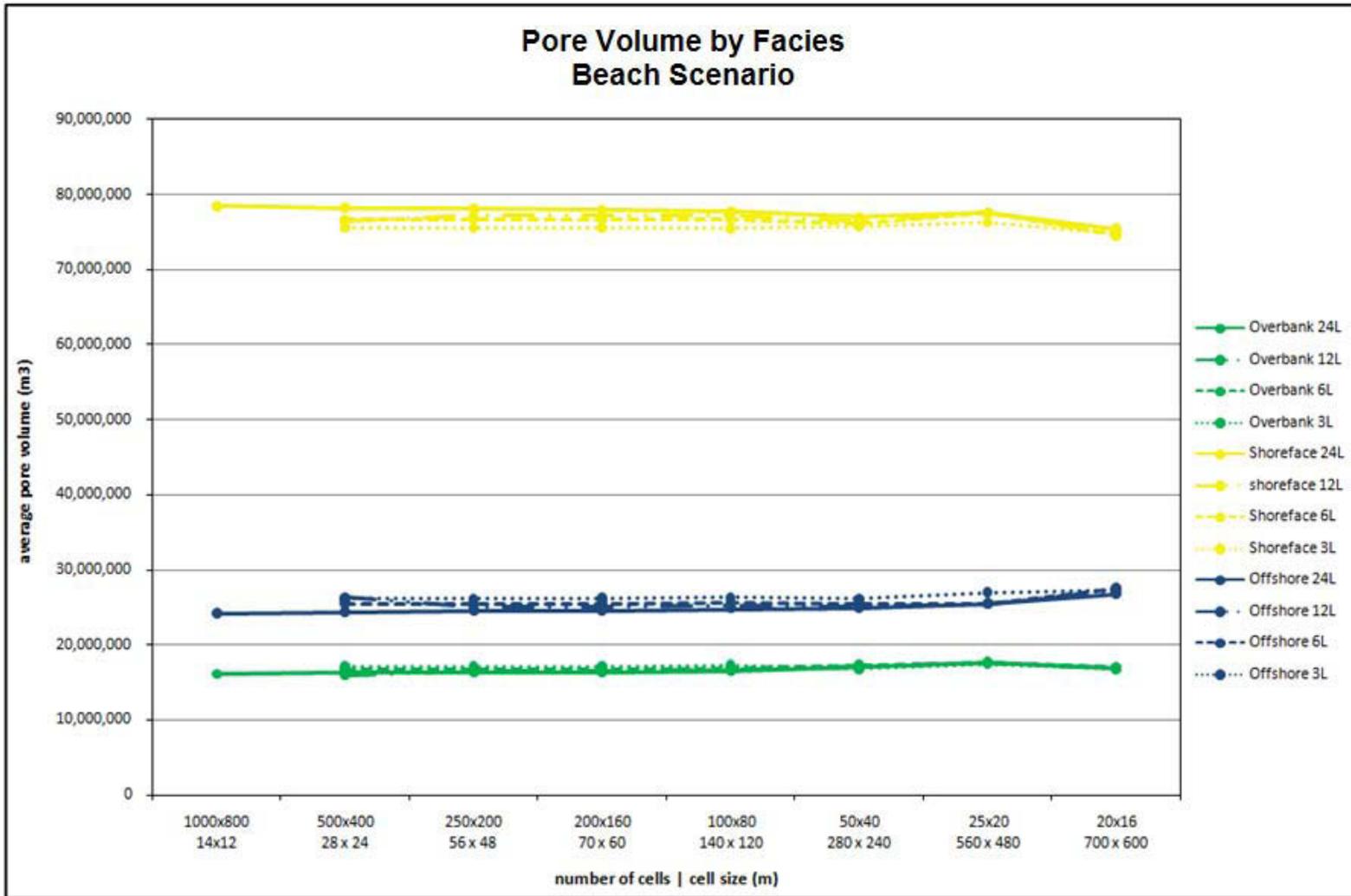
Figure 5.34. Average pore volume by facies - beach scenario. This scenario shows very little change to the pore volumes associated with each facies as the grids are upscaled vertically and horizontally. The subtle differences in the porosity distributions that are seen in Figure 5.24 result in changes in pore volume, relative to the base model, of less than 10%.
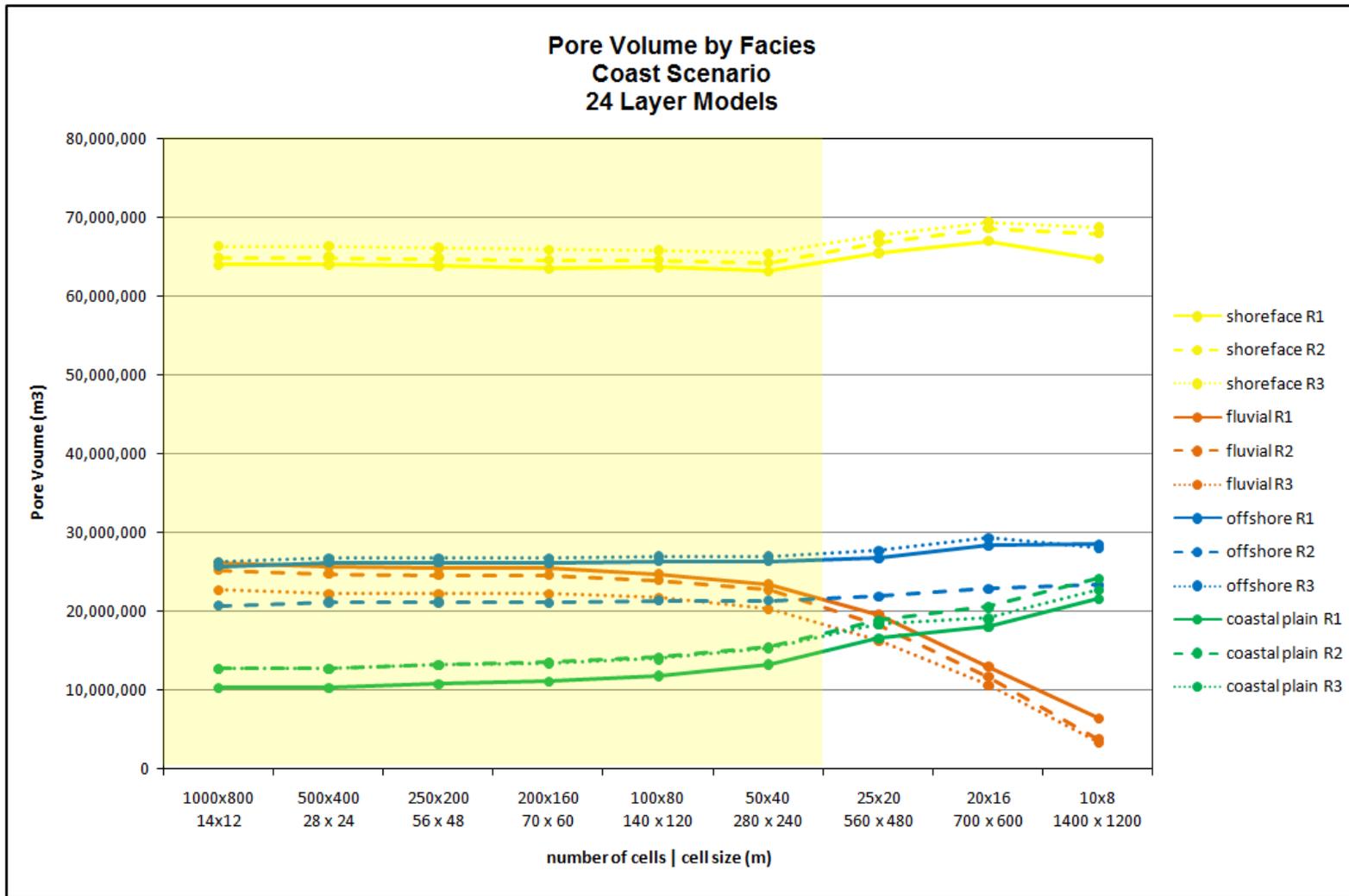
Figure 5.35. Multiple realizations of pore volume of facies in a coast scenario. As with the channel models, there is only minor difference in the pore volumes associated with each facies between different realizations. The yellow shading highlights the grids where the cell size is less than the channel width.
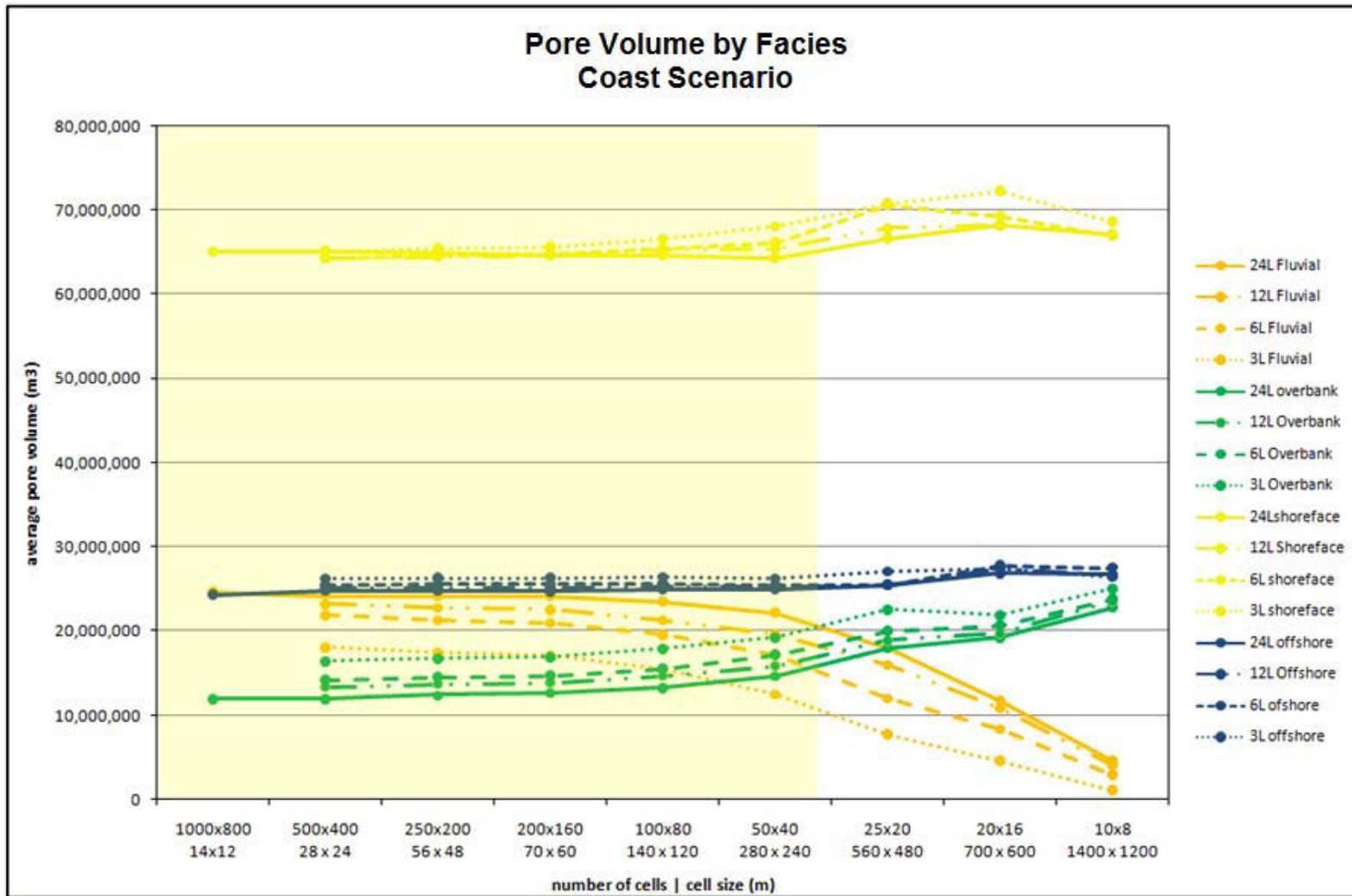
Figure 5.36. Changes to the average pore volume of the facies in the coast scenario with vertical upscaling. This diagram indicates that the offshore and shoreface facies are relatively insensitive to the effects of vertical upscaling. The fluvial facies is affected by vertical upscaling at all grid cell sizes. The changes in the overbank facies are most likely to be the result of redistribution of the fluvial facies into the overbank facies. In this scenario the channels have a mean thickness of 2 m—the average layer thickness in the 6-layer model. There is a big drop in the pore volume associated with the channel facies between the 6-layer model and the 3-layer model, which has an average thickness of 4m. The yellow shading highlights the grids where the cell size is less than the channel width.
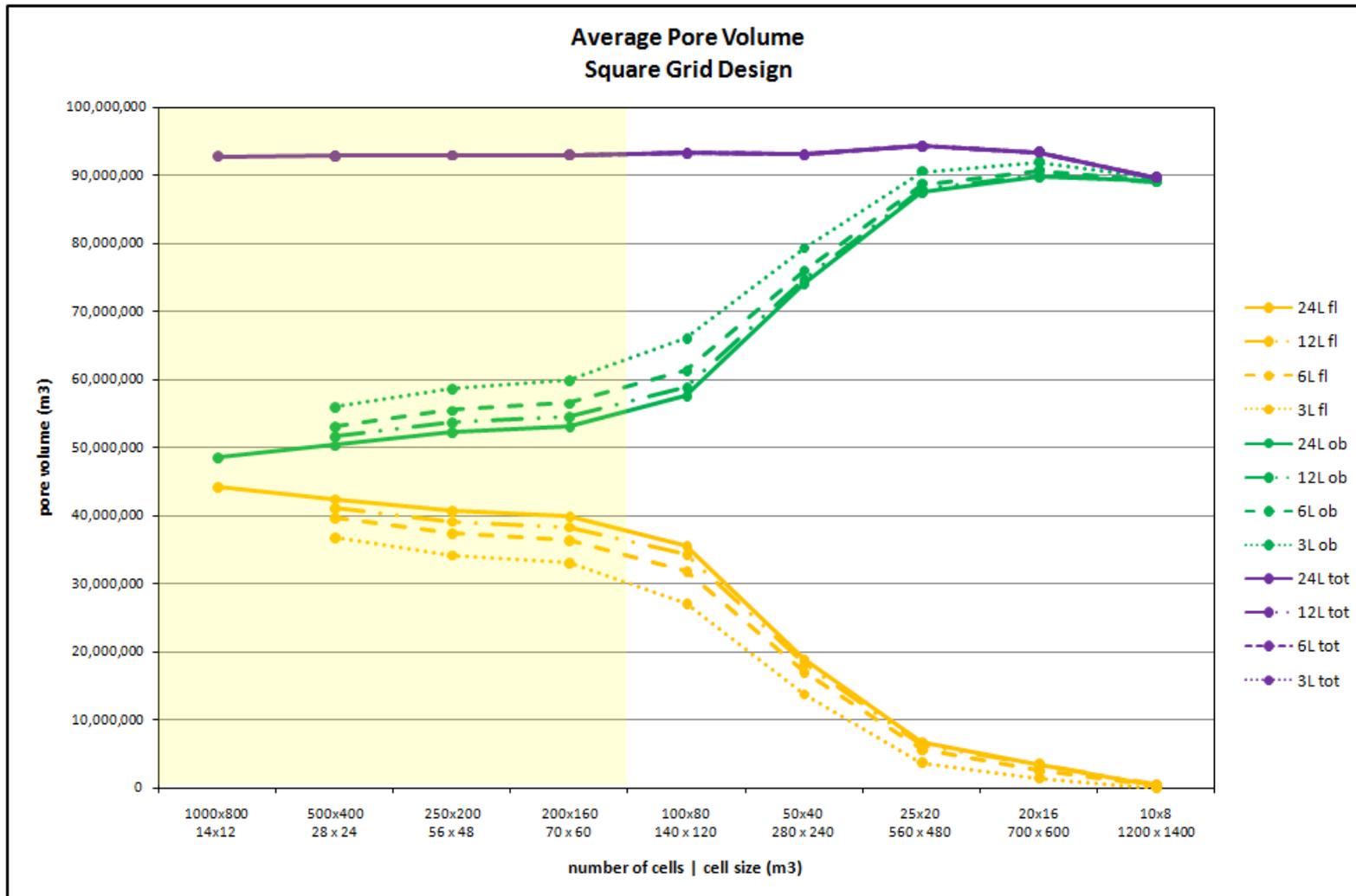
Figure 5.37. The impact of vertical upscaling on average pore volume, SQ 100-25 scenario. Although the total pore volume for the grids is unaffected by vertical upscaling, there are differences in the pore volume associated with each facies. The differences are greatest when the channel facies is well preserved, and they diminish as the channel facies is 'averaged out'. The loss of high and low end members and the trend towards normalizing the distribution shown the porosity distribution (for example Figure 5.18 produce the differences in pore volume shown here. The yellow shading highlights the grids where the cell size is less than the channel width.
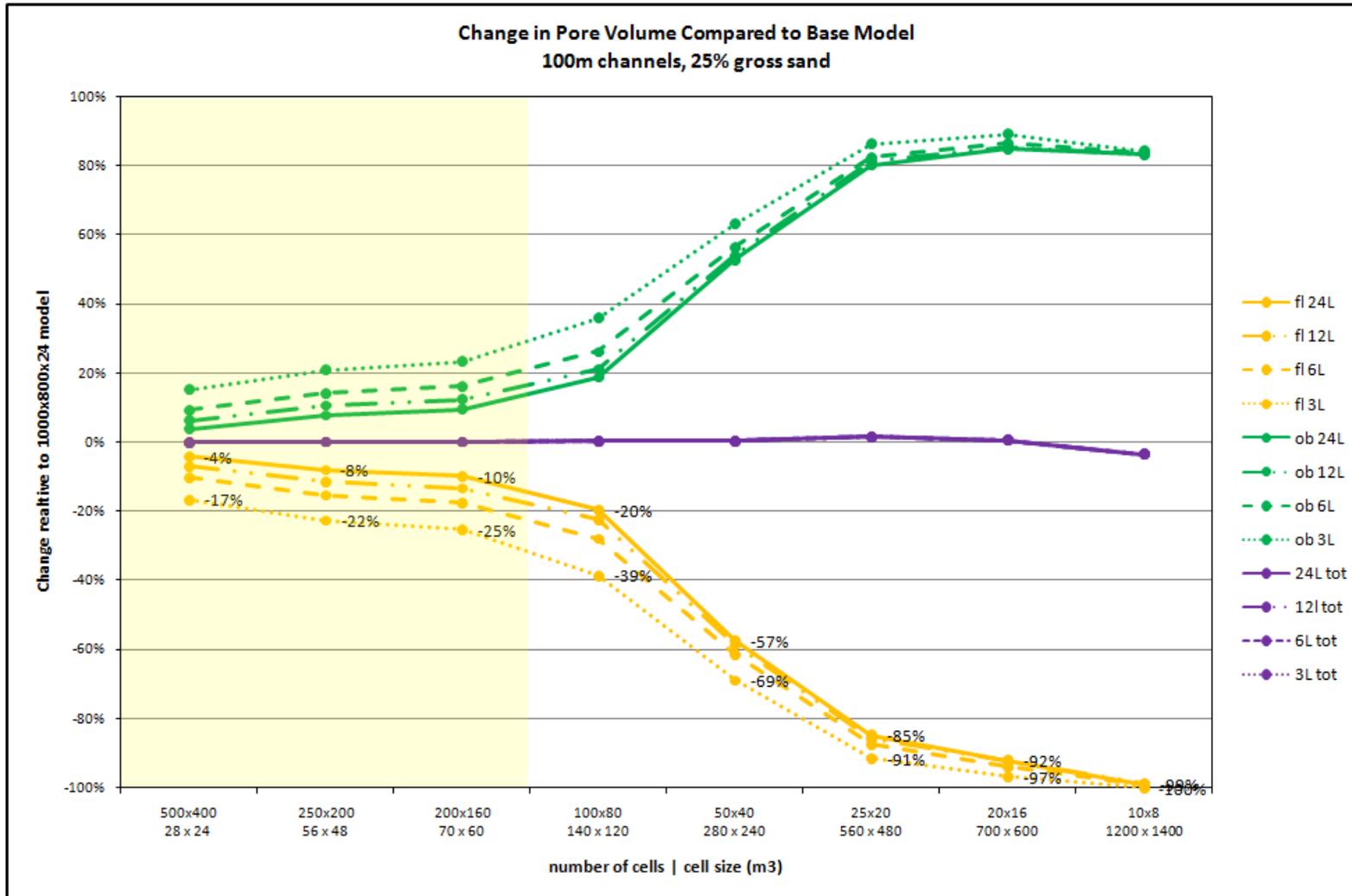
Figure 5.38. Change in average pore volume relative to base model. SQ 100-25 scenario. The amount of pore volume lost due to horizontal upscaling does not change significantly (<10%) until the grid cell size exceed the channel widths (points within yellow shading). Vertical upscaling of the grid can cause a loss of pore volume of between 5-15% for grids whose cells do not exceed the width of the channels. Once the cell width exceeds the channel width, horizontal upscaling has a far greater impact on pore volume by facies than vertical upscaling. The total amount of pore volume in the model is virtually unaffected by upscaling.
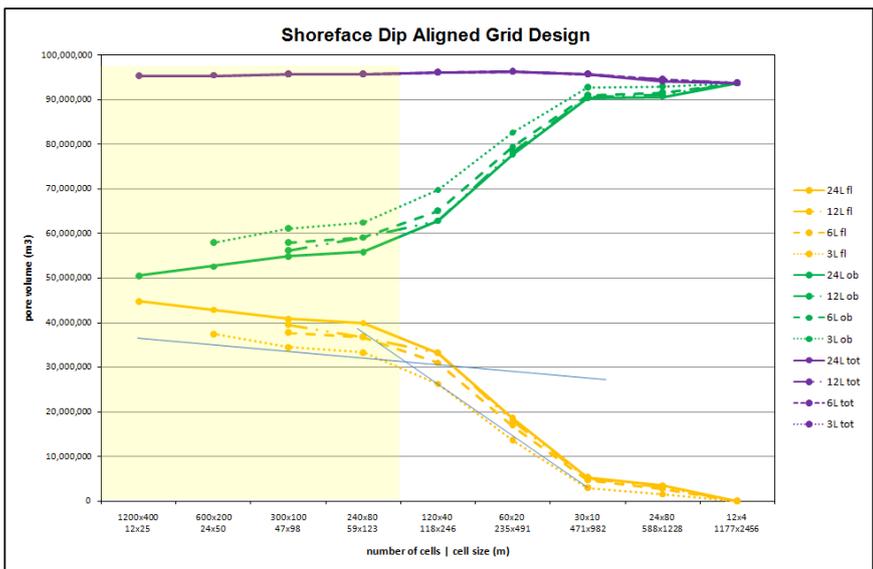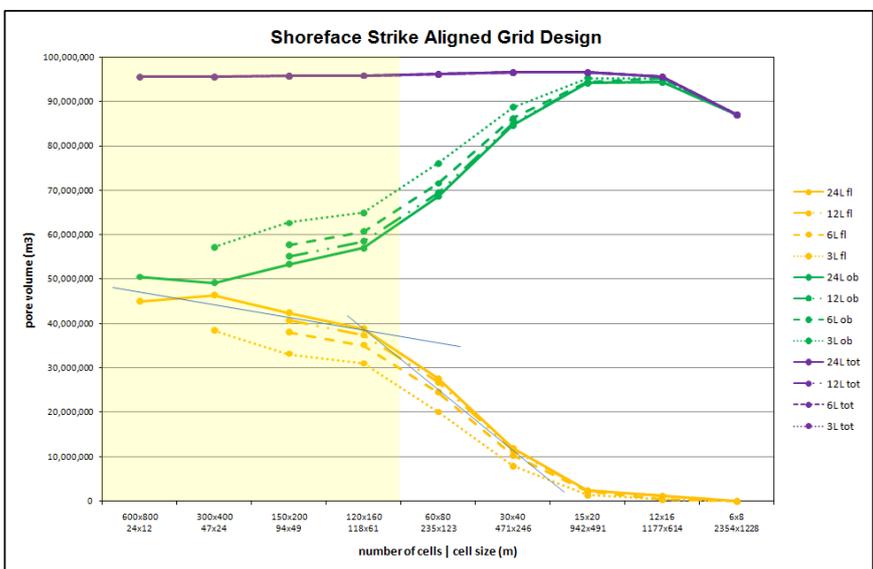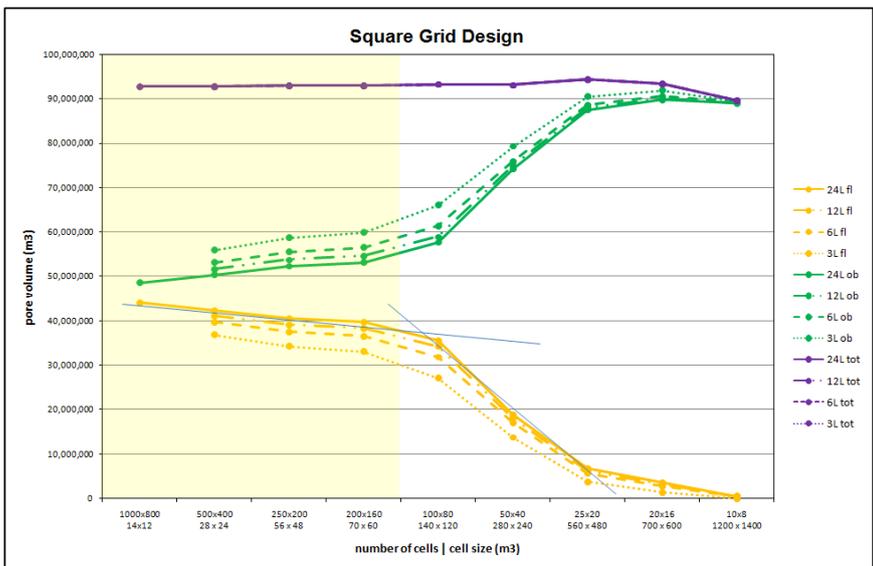
Figure 5.39. Pore volume by facies. 280-25 scenario - all grid designs. Realizations 1-3. The yellow tint highlights the grids that have cell sizes smaller than the width of the channels. All grid designs show a significant change in rate of change of pore volume as the grids are upscaled once the cell size exceeds the channel width (280 m). The curves have two trends (blue lines) that usually intersect at the point at which the channel width is more than half the cell width. Although all models have the same total pore volume, vertical upscaling produces a change in the distribution of pore volume for each horizontal grid design.
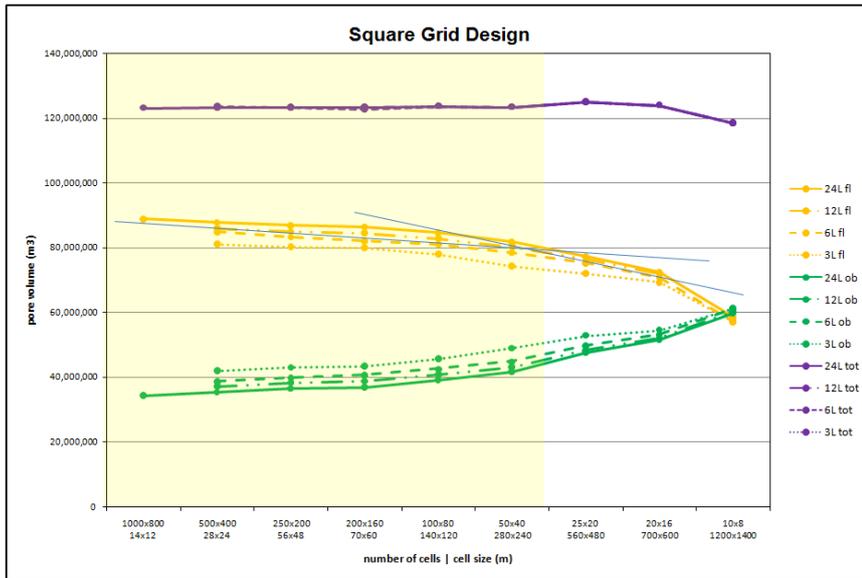
Figure 5.40. Pore volume by facies. 280-50 scenario - all grid designs. Realizations 1-3. The yellow tint highlights the grids that have cell sizes smaller than the width of the channels. All grid designs show a change in rate of change of pore volume as the grids are upscaled once the cell size exceeds the channel width (280 m).
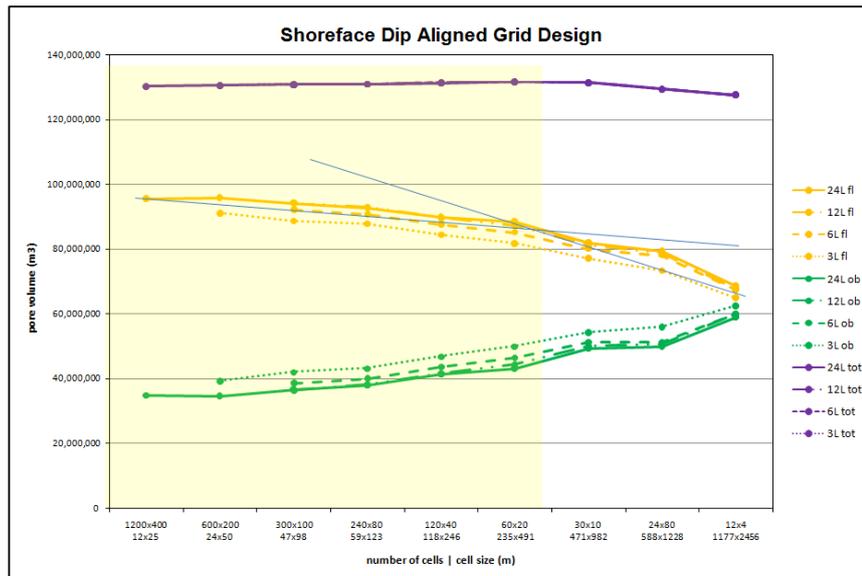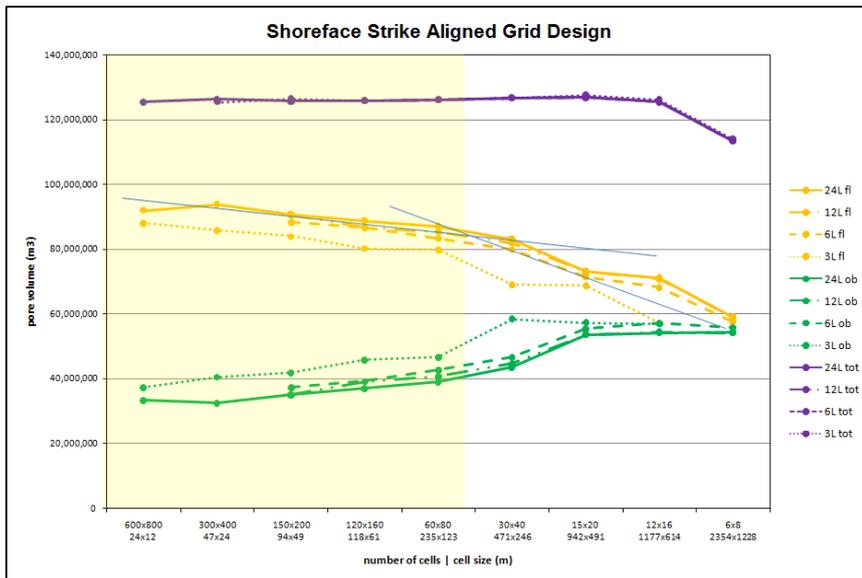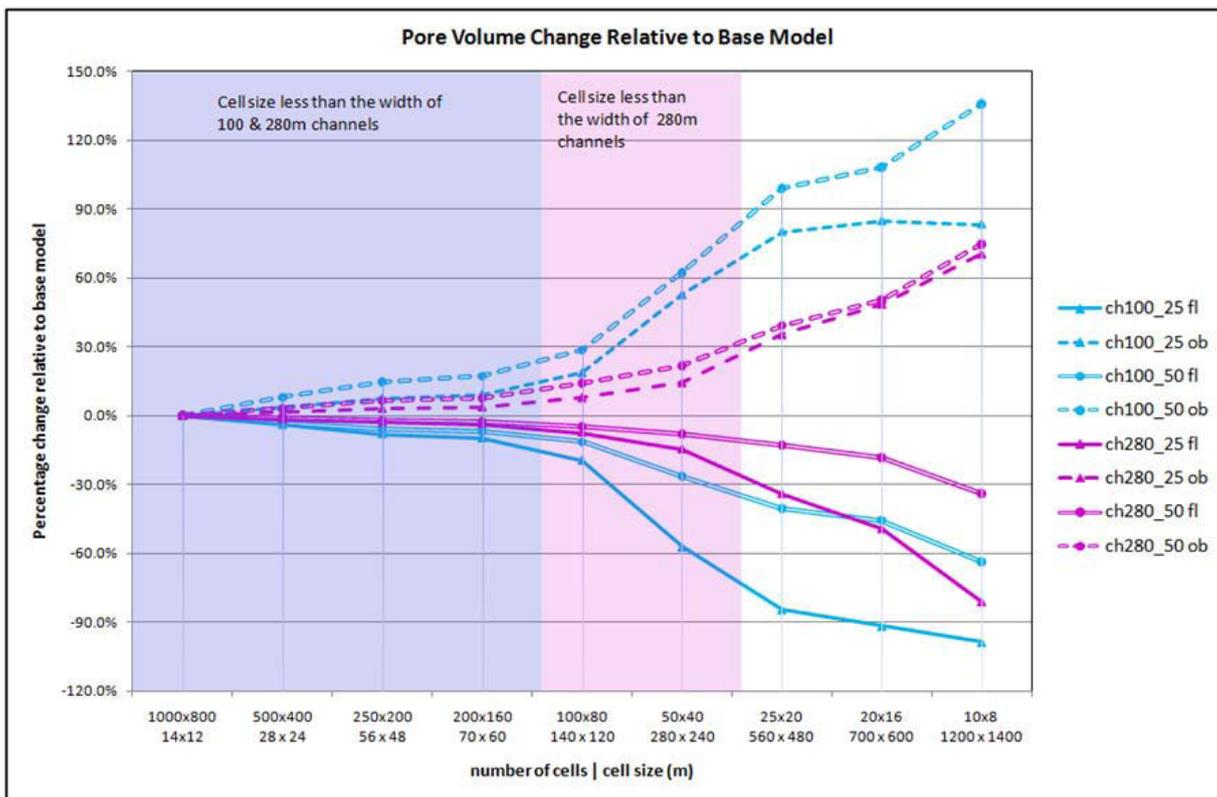
Figure 5.41. Change in facies pore volume relative to base model. Square grid, 24 layers, all channel scenarios. This shows that the 100 m channel models undergo the largest shift in pore volumes once the channel width is exceeded. Although more subtle, a change in the curves associated with the 280 m channels also change gradient once the cell widths are greater than the channel widths.
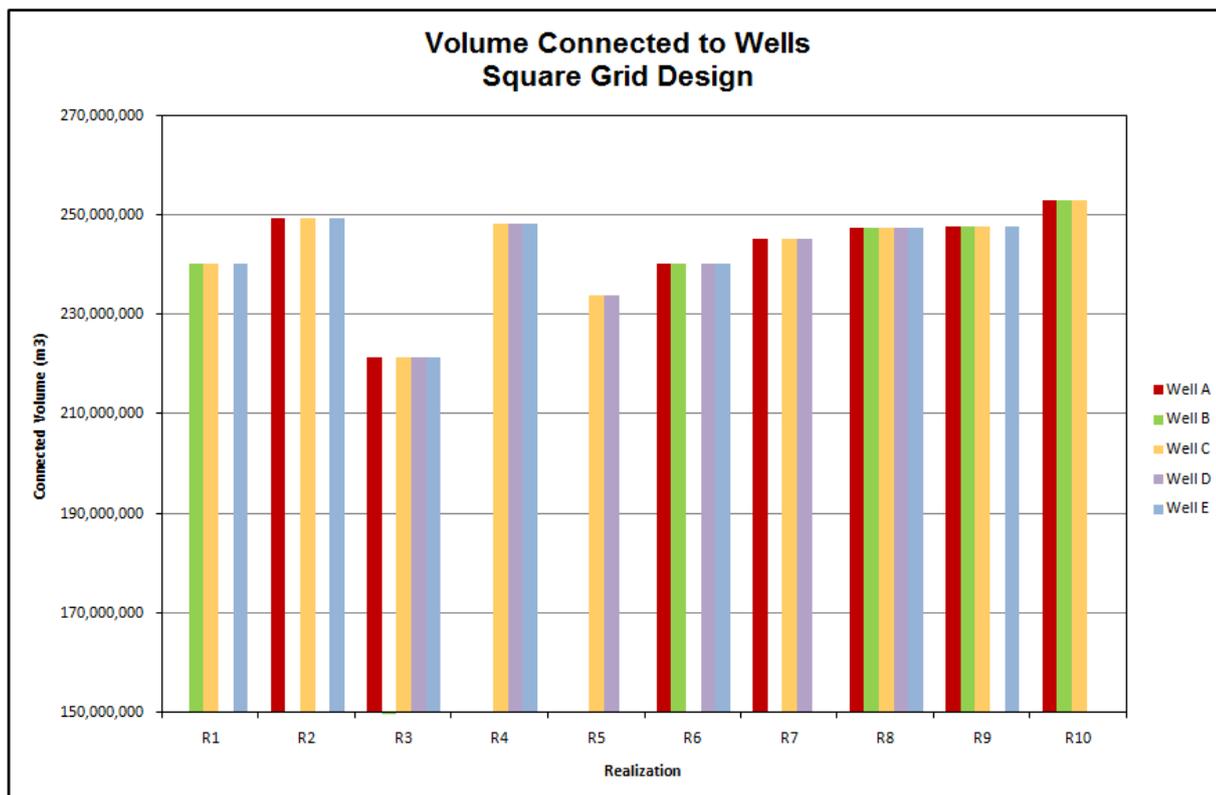
Figure 5.42. Volume of channel facies connected to wells –SQ 280-25 scenario. 100 x 800 x 24 grid. 10 realizations (R1-R10). Where wells penetrate a sandbody, each well in a realization is seeing the same volume as the other wells. This indicates that in the base model, all sandbodies are connected.
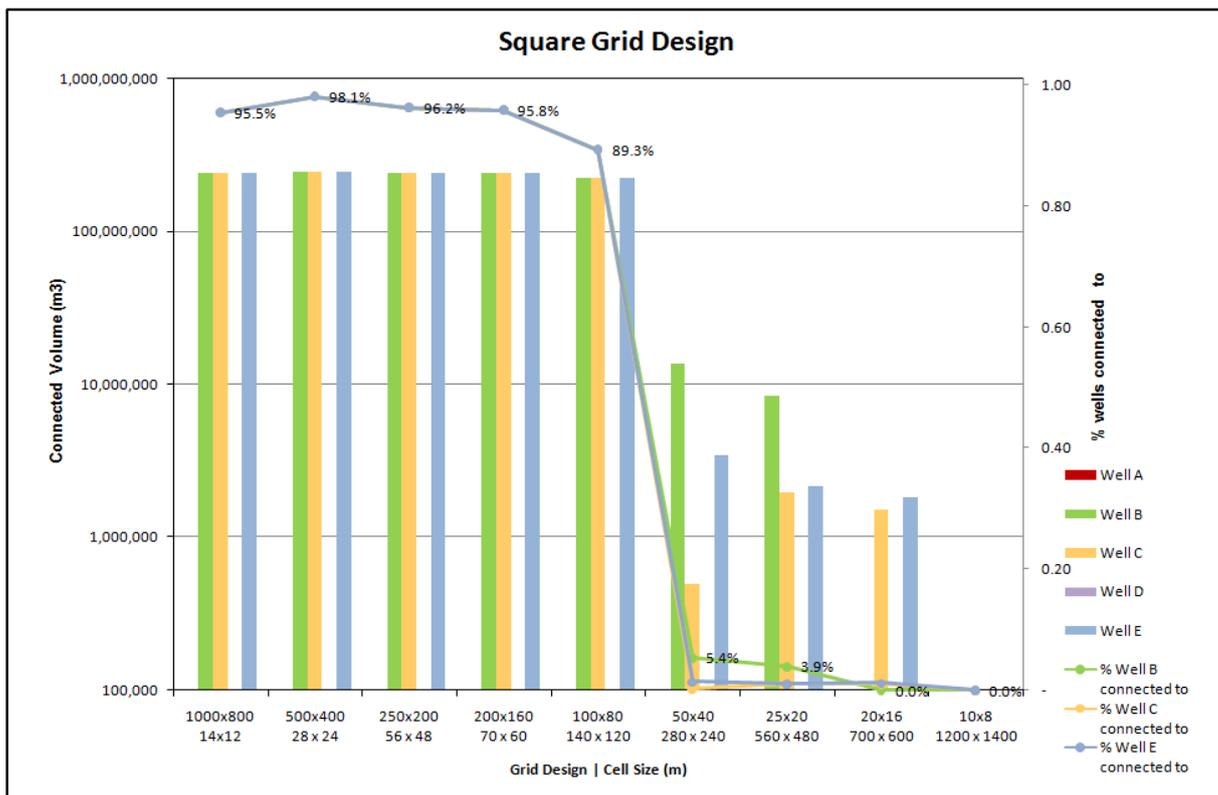
Figure 5.43. Volume of fluvial facies connected to wells, SQ280-25 scenario. Realization 1. Once the cell width exceeds half the channel width, the connectivity of the channel facies decreases and the wells no longer all see the same volume. Note, in order the display the detail of the variability in volumes once the vertical scale on this plot is logarithmic. Figure 5.44 shows the proportion of channel facies that the wells connect to.
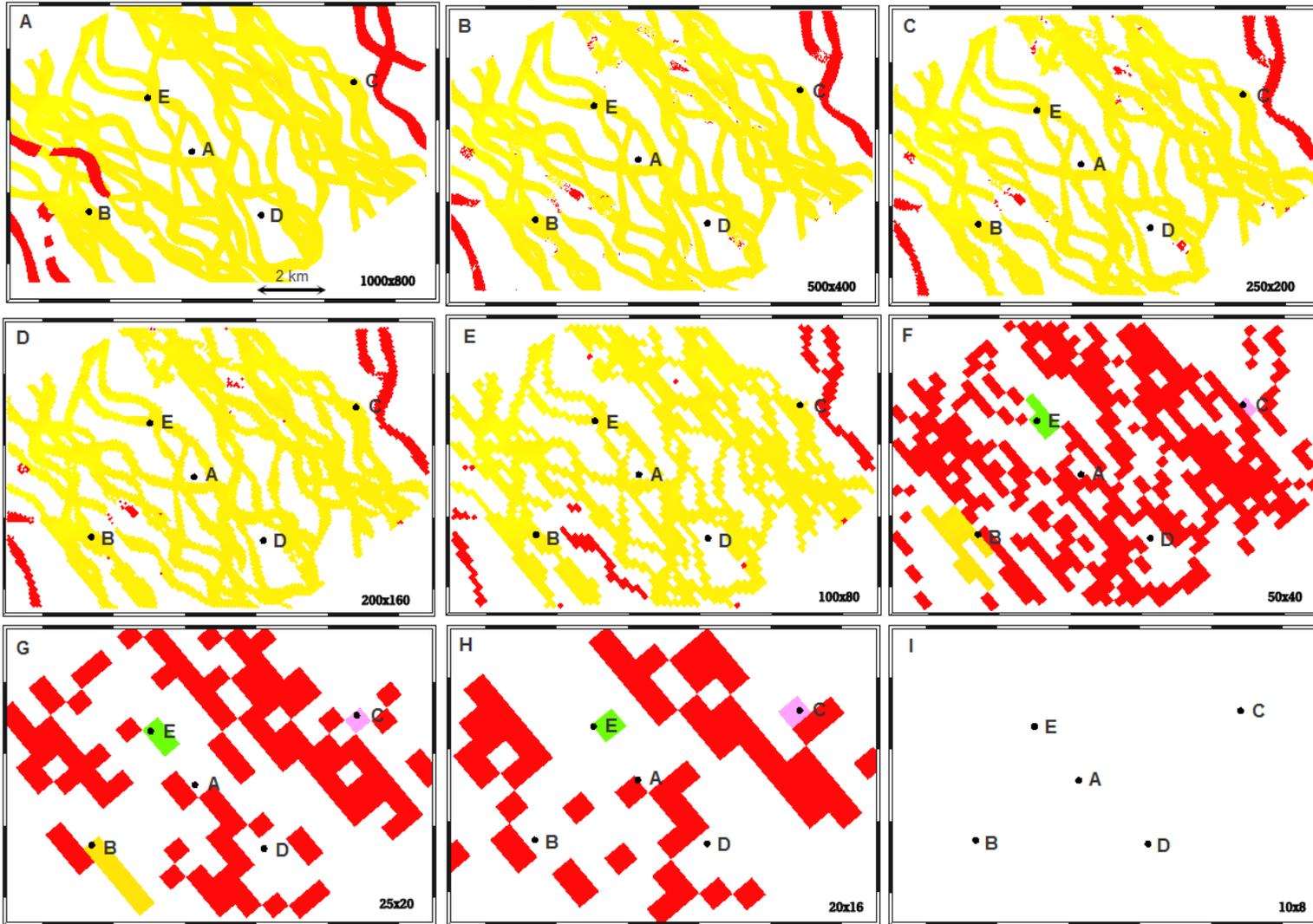
Figure 5.44. Fluvial facies connectivity to wells—3 layers (except for 1000 x 800 grid which is 24 layers). These plots show all the fluvial facies in the SQ 280-scenario. Red cells are fluvial facies not connected to any wells. Other colours indicate connectivity to wells. In diagrams A to E wells B, C, & E are connected to the same volume (yellow). Wells A and D are not connected to channel facies. Once the cell size exceeds half the channel width (50 x 40 grid), the connectivity of the channels to the wells begins to decrease rapidly.

A: Tidal channel (1) cutting through shoreface sediments (2) of a barrier island.

B: Theoretical grid cells, 0.5 m thick.

C: Vertical upscaling of grid cells to 1 m thick.

D: Vertical upscaling to 1.5 m thick.
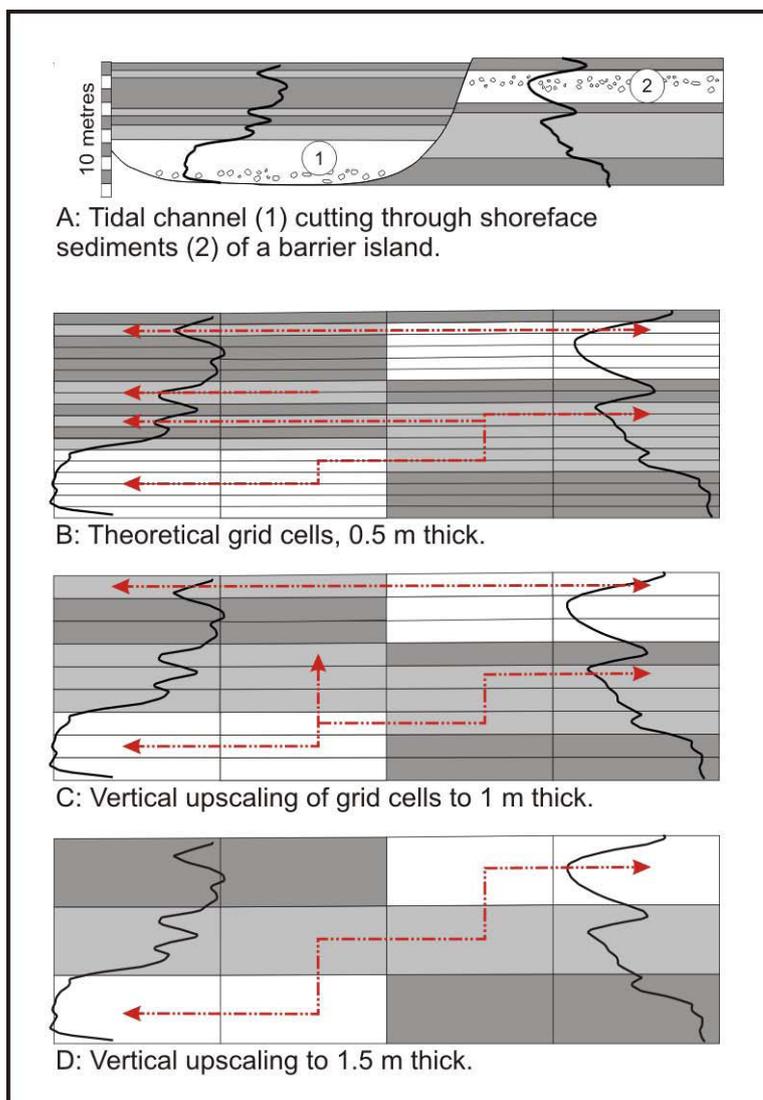
Figure 5.45. The impact of vertical averaging on facies connectivity between a tidal channel and upper shoreface. Upscaling has the potential to increase the connectivity between the tidal channel (1) and the upper shoreface (2). The colour of the blocks is an indication of the lithology, and hence porosity/permeability. White blocks are sandstone, pale grey blocks are sandy shale and dark grey blocks are shale. Flow is possible through the white and pale grey blocks, but not through the dark blocks which would be modelled as non-reservoir. In this example, flow is not possible through the corner of cells, thus only in the final stage (D) can fluid flow between the two sandbodies.

Care also needs to be taken during vertical upscaling to ensure that thin features, such as shale layers, shale drapes and high permeability streaks, which can play an important role in vertical fluid flow are not upscaled out of existence. From (Riordan et al., 2008).
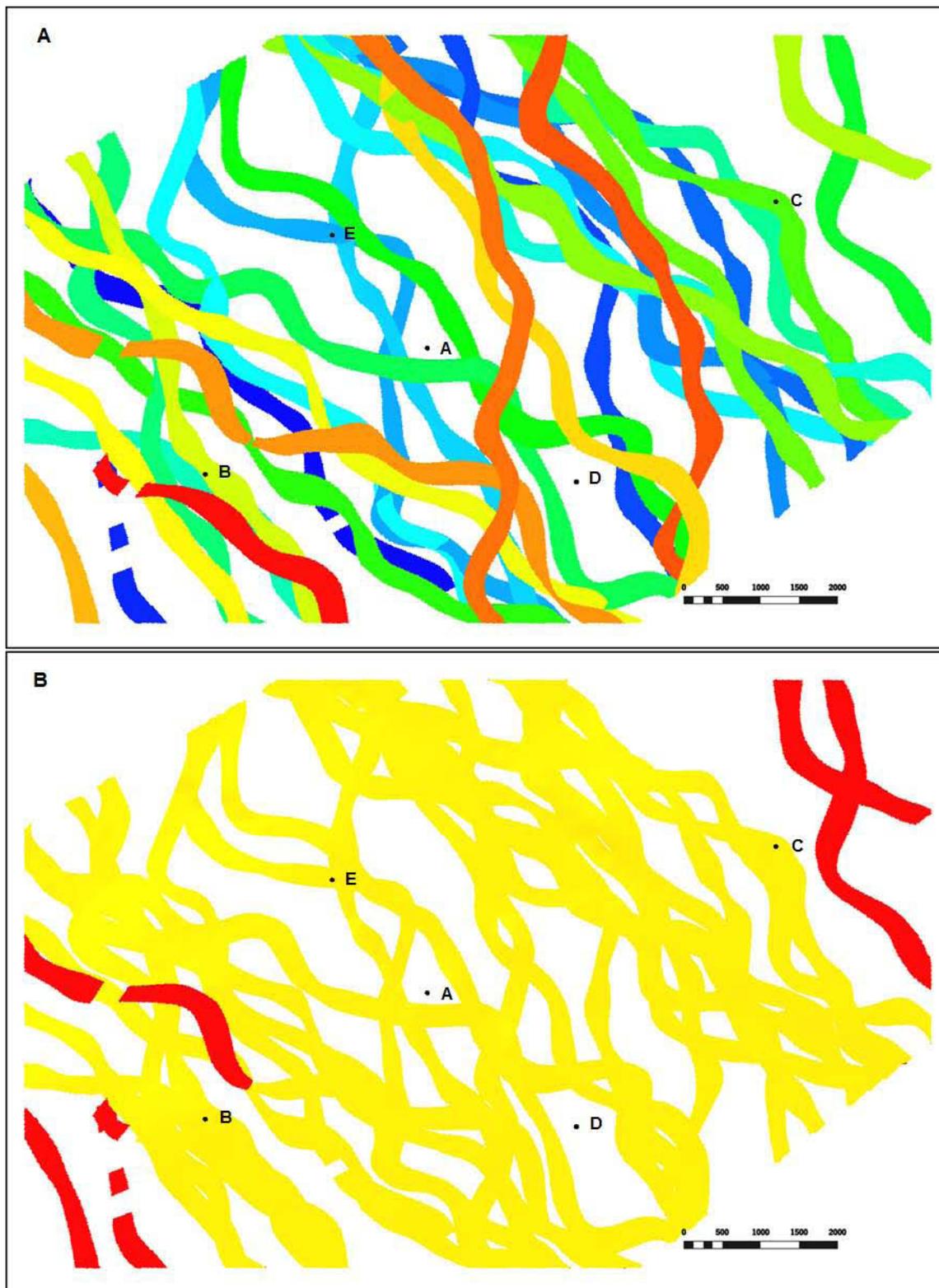
Figure 5.46. All channel bodies in the SQ280-25 scenario (realization 1). The top figure (A) shows the individual channel bodies. The lower figure (B) shows the channels that are connected to the wells (yellow is connected). The wells that are connected to the channels are Wells B,C and E. These wells all see the same volume of channel sands, which is approximately 95% of the total volume of channels in the model. As can be seen in figure A, the sinuosity and angle of the channels is the likely cause of the high level of connectivity.